"In presenting the dissertation as a partial fulfillment of the requirements for an advanced degree from the Georgia Institute of Technology, I agree that the Library of the Institution shall make it available for inspection and circulation in accordance with its regulations governing materials of this type. I agree that permission to copy from, or to publish from, this dissertation may be granted by the professor under whose direction it was written, or, in his absence, by the dean of the Graduate Division when such copying or publication is solely for scholarly purposes and does not involve potential financial gain. It is understood that any copying from, or publication of, this dissertation which involves potential financial gain will not be allowed without written permission.

_____

_____

THE TRANSIENT RESPONSE CHARACTERISTICS OF SIMULATED PNEUMATIC PLUMBING SYSTEMS WHEN SUBJECTED TO SHOCK WAVE INPUTS

A THESIS

Presented to

the Faculty of the Graduate Division

by

George W. Stone

In Partial Fulfillment

of the Requirements for the Degree

Master of Science in Aeronautical Engineering

Georgia Institute of Technology

May, 1960

THE TRANSIENT RESPONSE CHARACTERISTICS OF SIMULATED PNEUMATIC PLUMBING SYSTEMS WHEN SUBJECTED TO SHOCK WAVE INPUTS

Approved:

Date Approved by Chairman: July 8, 1960

ACKNOWLEDGMENTS

The author expresses his appreciation to Doctors Arnold L. Ducoffe and Frank M. White, Jr. for suggesting the subject and giving invaluable assistance through all phases of work. Gratitude is also extended to Doctor C. W. Gorton for his critical review of the topic and to Messrs. G. W. D. Cook, J. Van Tassel, G. L. Lattal and G. W. Brown for their assistance in making the apparatus and in conducting the tests.

Sincere appreciation is extended to the Sandia Corporation for the financial and material aid which made this work possible.

TABLE OF CONTENTS

LIST OF TABLES

LIST OF FIGURES

LIST OF SYMBOLS

a	Ratio of straight-through fitting I.D. to tubing I.D.
A	Cross-sectional area of tube
C	Constant
d	Derivative
D	Diameter of tube
f	Local friction factor
$\bar{f}$	Mean friction factor
f^*	Pseudo friction factor
I.D.	Inside diameter
K	Parameter for transient laminar flow $\left(\frac{\text{inches}}{\text{lb sec}}\right)^2$
L	Length of tube
m	Mass of gas in the system
m'	Rate of mass flow $\left(\frac{dm}{dt}\right)$
M	Parameter for transient turbulent flow $\left[\left(\frac{\text{inches}}{\text{lb}}\right)^2\right]^{0.5263} \frac{1}{\text{sec}}$
N	Exponent
p	Pressure
P_I	Pressure inside upstream end of tube
P_{II}	Pressure inside downstream end of tube
P_1	Pressure outside upstream end of tube
P_2	Pressure outside downstream end of tube
$\bar{p}$	Mean pressure in the system
P_i	Transient input pressure

P_r	Transient response pressure
$P_{i_{max}}$	Maximum input pressure
$P_{r_{max}}$	Maximum response pressure
$P_i(t)$	Transient input pressure
$P_r(t)$	Transient response pressure
P_r'	Derivative of response pressure $(\frac{dP_r}{dt})$
$P_r'(t)$	Derivative of response pressure $(\frac{dP_r}{dt})$
$P_r(t + \Delta t)$	Transient response pressure at time $t + \Delta t$
$P_r'(t + \Delta t)$	Derivative of response pressure at time $t + \Delta t$
psia	Pounds per square inch absolute
psig	Pounds per square inch gauge
R	Gas constant
Rey	Tube Reynolds number = $\frac{wD}{A\mu}$
T	Absolute temperature
t	Time
Δt	Increment of time
U	Mean velocity through any cross-section of tube
V	Total volume of system
V_s	Volume of response part of system
w	Rate of mass flow
x	Spatial co-ordinate
μ	Coefficient of absolute viscosity
π	Constant (= 3.1416)
ρ	Mass density of gas

Φ	Geometric parameter for laminar flow
Ψ	Geometric parameter for turbulent flow $(\text{inches})^{-0.9421}$
τ_w	Wall shearing stress

SUMMARY

The purpose of this investigation was to determine the response characteristics of simulated missile pressure-sensing systems subjected to shock-type pressure input functions.

The systems consisted of a length of constant area tubing connected in series to a sensing volume. In addition, the effect of adding straight-through fittings at the tube extremities was also investigated. All combinations of four tubing lengths (1, 5, 10 and 15 feet), four tubing inside diameters (0.114, 0.182, 0.242 and 0.370 inches) and three receiver volumes (10.5, 53.7 and 106.7 cubic inches) were tested. The straight-through fittings had inside diameters varying from 50 to 100 per cent of the tubing diameter.

The shock wave inputs were generated by a shock tube and the wave strengths varied from 30 to 700 psig. Each geometric configuration of the typical system was subjected to the complete range of shock wave strengths.

The experimental results show the qualitative effects of the system geometric dimensions on the attenuation of a shock-type input.

A semi-empirical theory was developed for one-dimensional, isothermal, quasi-steady laminar or turbulent flow. The resulting equations of motion are non-linear, ordinary, differential equations, each containing a parameter which is a function of the system geometry and the ambient temperature.

The semi-empirical theory was numerically integrated for several

geometric configurations (incorporating the 100 per cent straight-through fittings) and several shock inputs. The correlation of theory with experiment is shown to be good.

CHAPTER I

INTRODUCTION

Sensitive, pressure-sensing devices are carried by many modern missiles for the purpose of controlling components, determining velocity or altitude, or for arming and detonating an explosive warhead. These devices generally consist of a length of circular tubing connected in series to a downstream, pressure-sensing instrument having a finite volume reservoir.

Static pressure measuring systems used in missiles are subjected to transient pressure inputs dependent upon the particular pressure trajectory which the missile flies. This investigation considers the problem of predicting the response pressure in the pressure-sensing system for a somewhat different case of a transient pressure input which simulates the impingement of a shock wave on a missile static pressure surface port.

This situation of a transient shock-type pressure input would arise if an anti-missile missile exploded in the vicinity of a missile using a pressure-sensing system for guidance or control. The resulting shock wave impinging on the surface pressure port could pre-actuate, damage, or destroy the pressure-sensing instrument.

Previous investigations (References 1, 2 and 3) have established the qualitative effects of tubing length, straight-through fittings and receiver volume on the attenuation of waves propagating through a simulated pressure-sensing system. The shock wave strengths were varied

between 30 and 700 psig.

However, these investigations were concerned only with the maximum input and response pressures and the records were taken at low paper speeds, thus prohibiting a quantitative analysis of transient effects. The investigation presented herein consisted of re-running the tests performed in References 1, 2 and 3 in order to obtain records suitable for a transient study, thus determining the degree of correlation which exists between the proposed semi-empirical theory and the experimental data.

CHAPTER II

APPARATUS

The equipment used in the experimental investigation consisted of a high-pressure air supply, control panel, shock tube, test section, instrumentation, and firing system.

Compressed Air Supply.--High pressure air was provided by a four-stage air compressor, having a maximum output of 20 cubic feet per hour at a pressure of 3000 psi. The compressor was powered by a six-cylinder gasoline engine.

Control Panel.--The control panel (see Figure 1) consisted of six needle valves which were used to regulate the flow of air and the pressure level in the various parts of the system. Included in the control panel were two pressure gauges with full scale readings of 0-3000 psig and 0-1000 psig. The 0-3000 psig gauge was used to monitor the air pressure supplied by the compressor.

The 0-1000 psig gauge, which was marked in increments of two psig, was used to measure the pressure in the shock tube or in the test section when calibrating the instrumentation. All the valves and gauges were shock mounted on a sheet of plywood. A small vibrator was attached to the plywood sheet to minimize any error due to frictional forces present in the 0-1000 psig gauge. A 0.027 inch orifice was connected in series with the 0-1000 psig gauge to protect it from the shock of a premature detonation of the shock tube. This orifice could be by-passed when the danger of such a shock was absent.

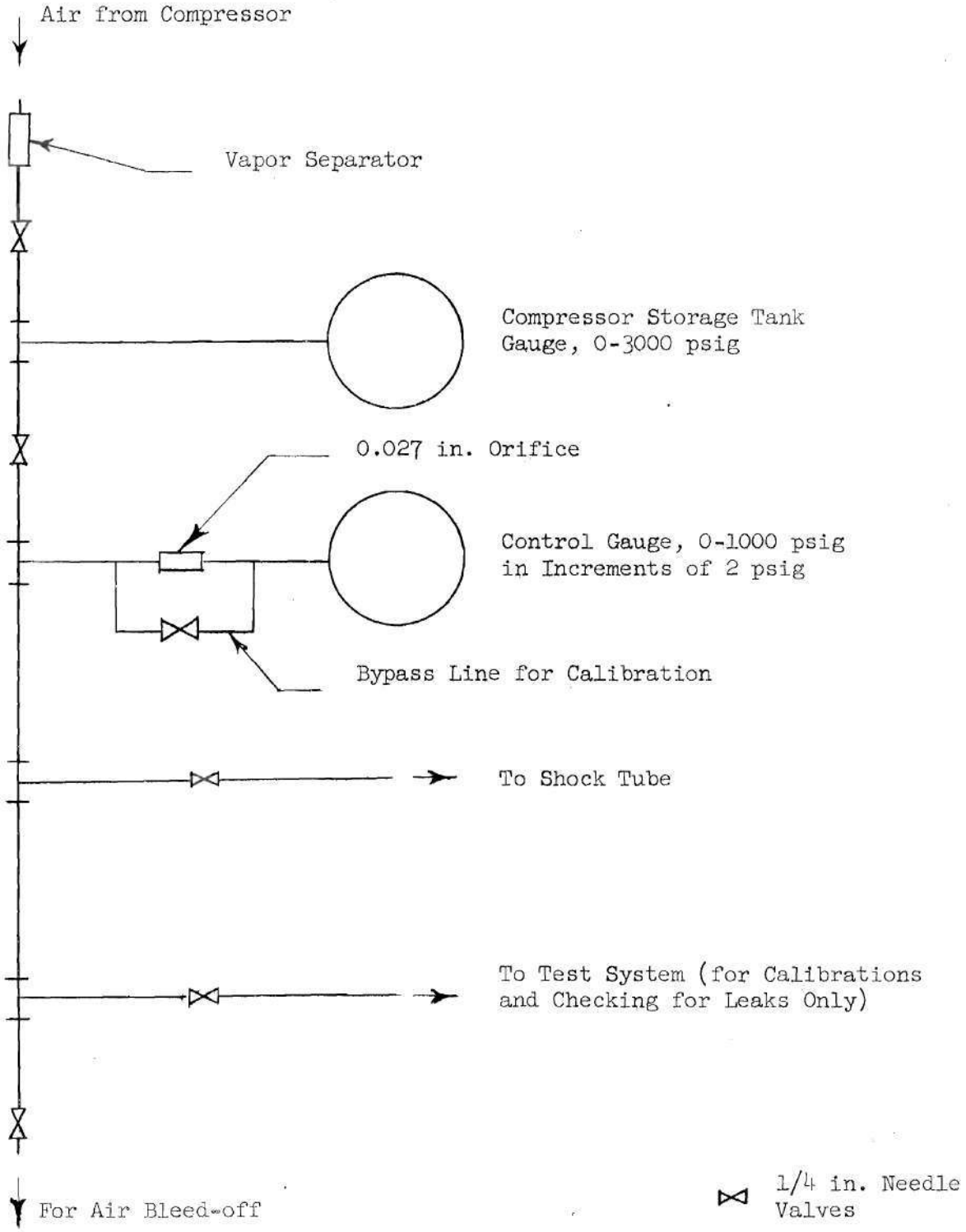

Fig. 1 Control Panel

Shock Tube.--The shock tube (see Figure 2) was constructed from a 7.63 foot length of high-pressure steel pipe with an outside diameter of 4.5 inches and an inside diameter of 3.5 inches. The pipe was sealed at one end with a steel plate which was fitted with a tubing connection for pressurizing the shock tube. The other end of the pipe was fitted with a steel nozzle with an inside diameter of 2.0 inches (see Figure 3).

The nozzle was removable so that a polyester film diaphragm could be inserted across the end of the shock tube. A 2-1/2 x 2-3/4 x 1/8 inch "O" ring gasket was used to maintain an airtight seal between the nozzle and the shock tube. The shock tube, excluding the nozzle, had an internal volume of 840 cubic inches.

The shock tube was securely mounted on a heavy hardwood table which was fastened to a reinforced concrete pad. The table was mounted so that it could recoil from the shock blast (see Figure 4). This was accomplished by shock-mounting the table with two heavy coil springs secured axially by 1/2 x 10 inch bolts to two ell brackets mounted on the concrete pad. The table was permitted to recoil longitudinally against the springs, but was prevented from moving laterally or vertically by the ell brackets and by two 1/8 inch steel guy wires. Proper adjustment of the spring tension in the guy wires permitted the table to return to its initial position after each blast.

Test Section.--The test section consisted of a pick-up tube, a test line, straight-through fittings, and a receiver volume (see Figure 5).

The pick-up tube was used to direct the center portion of the shock wave into the simulated missile plumbing system. It consisted of a 0.56 inch inside diameter steel tube mounted on the concrete pad (see

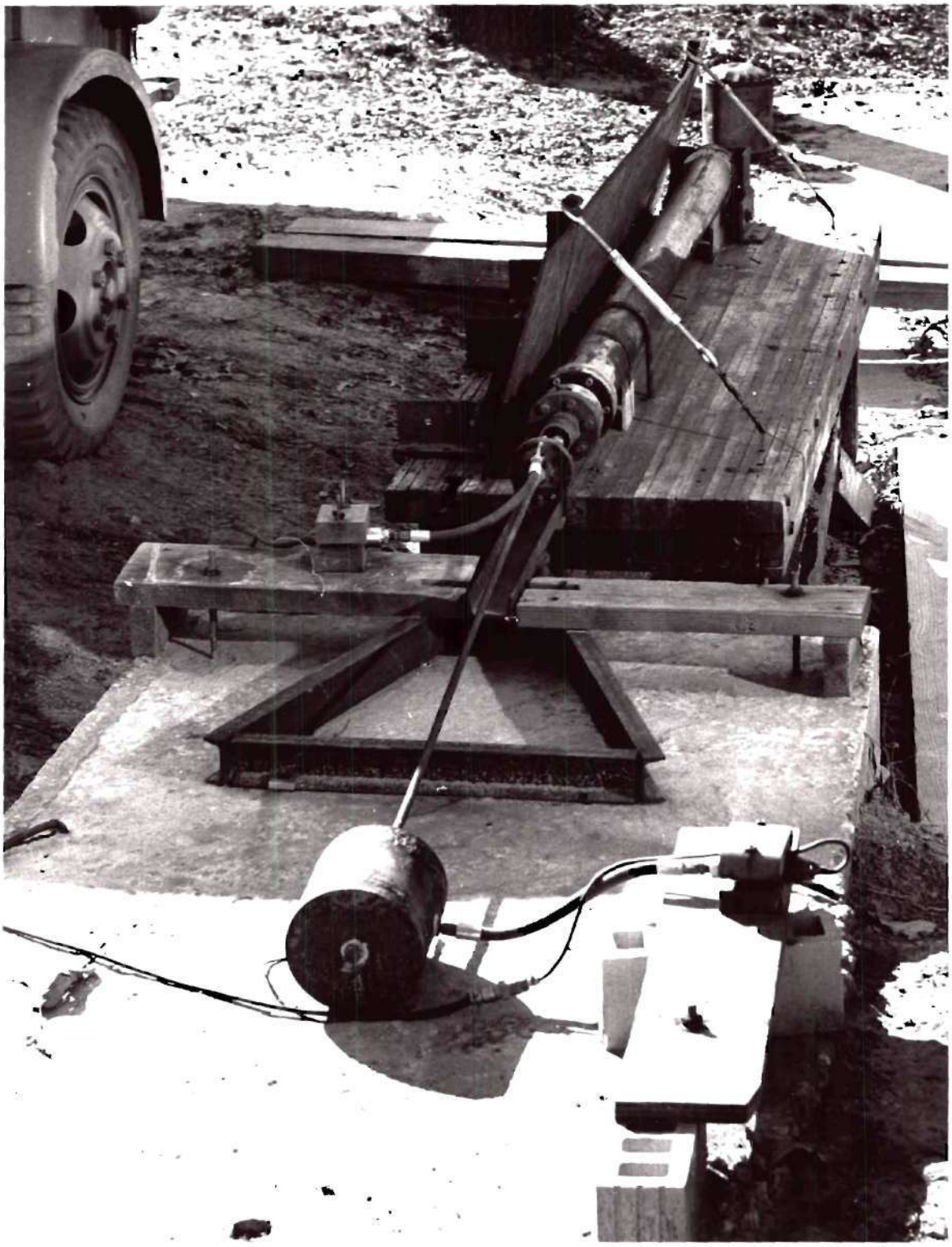

Fig. 2. Shock Tube and Test Area

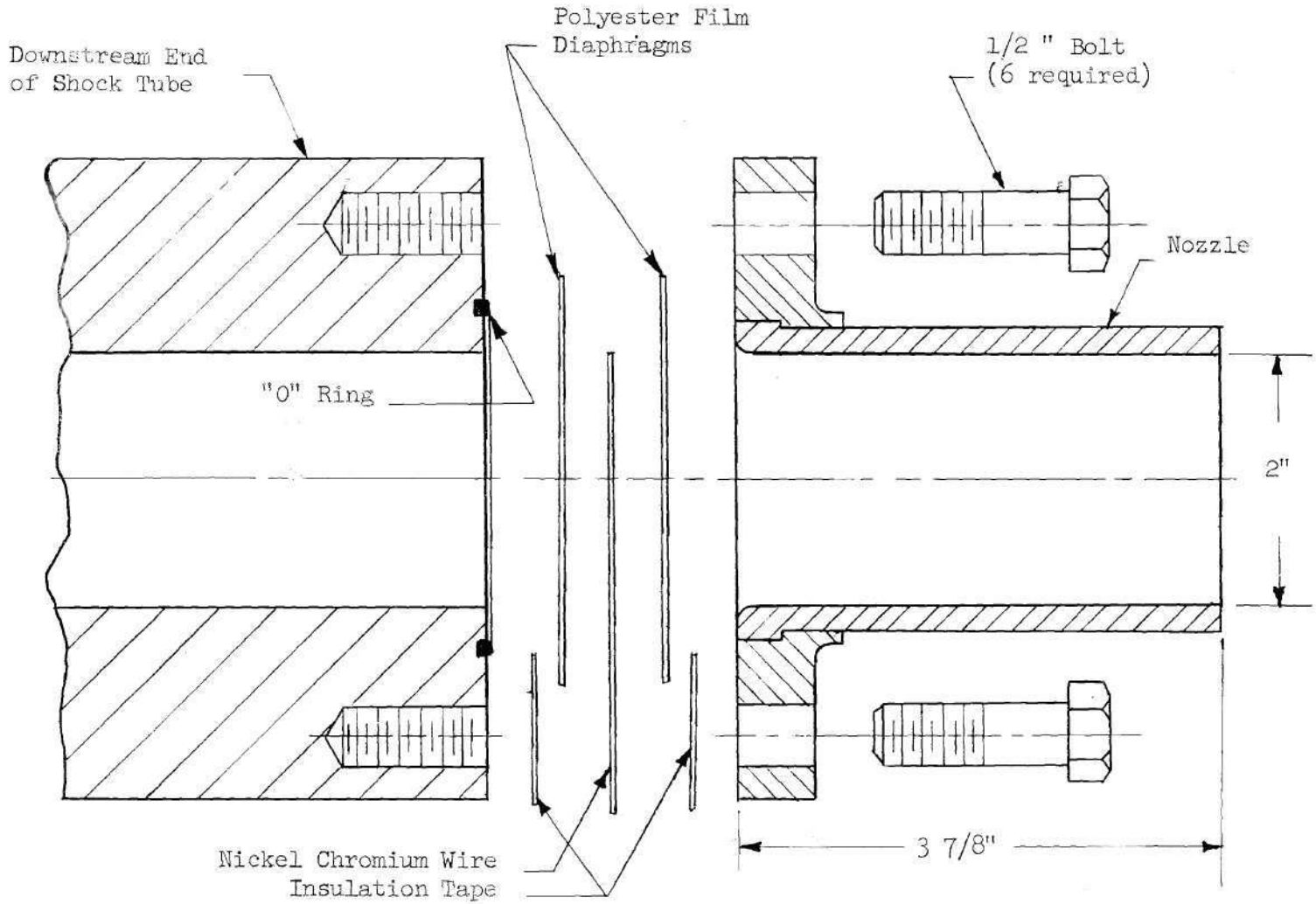

Fig. 3 Detail of Nozzle

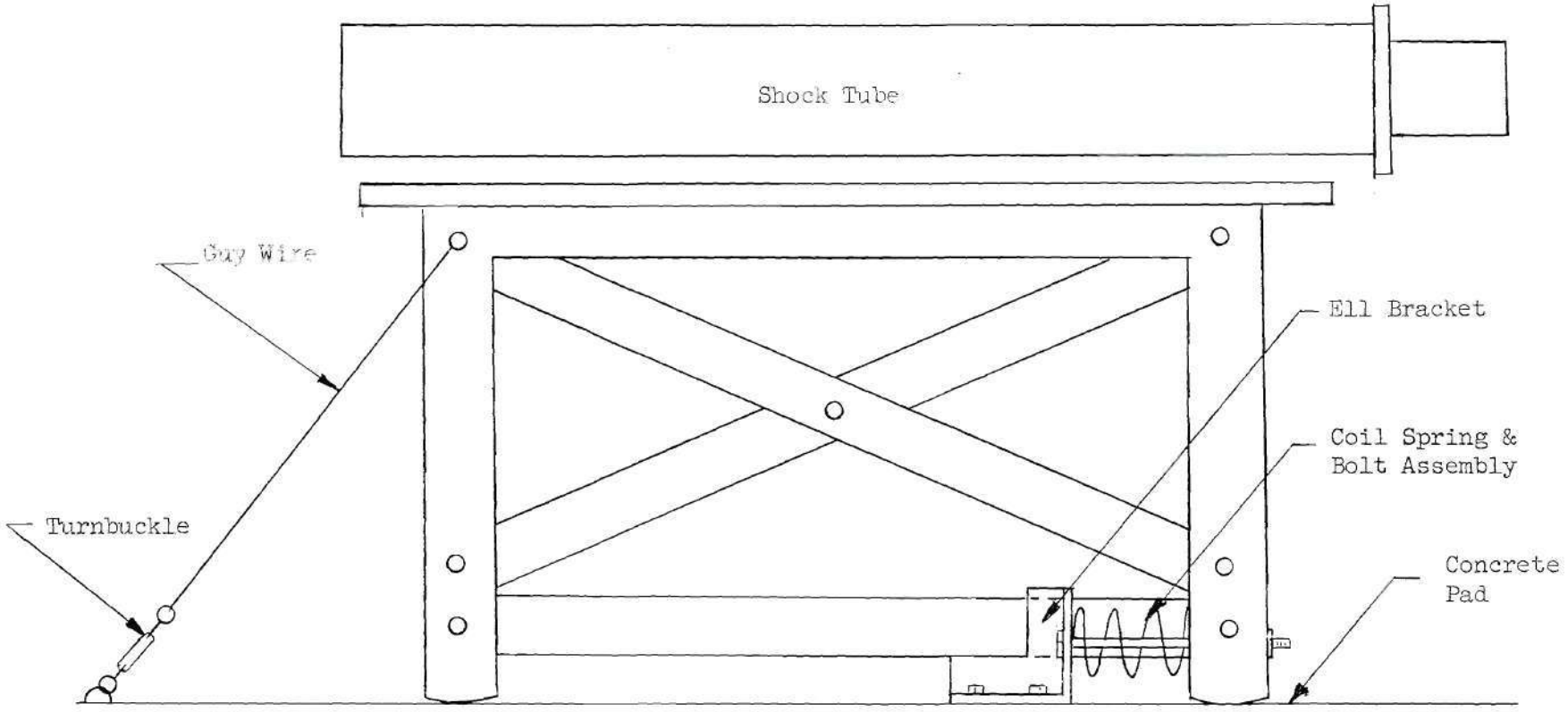

Fig. 4 Table Mounting

Note: Fittings HBTX-S-8 for 0.370 in. and 0.182 in. Line I.D.

Fittings HBTX-S-5 for 0.242 in. and 0.114 in. Line I.D.

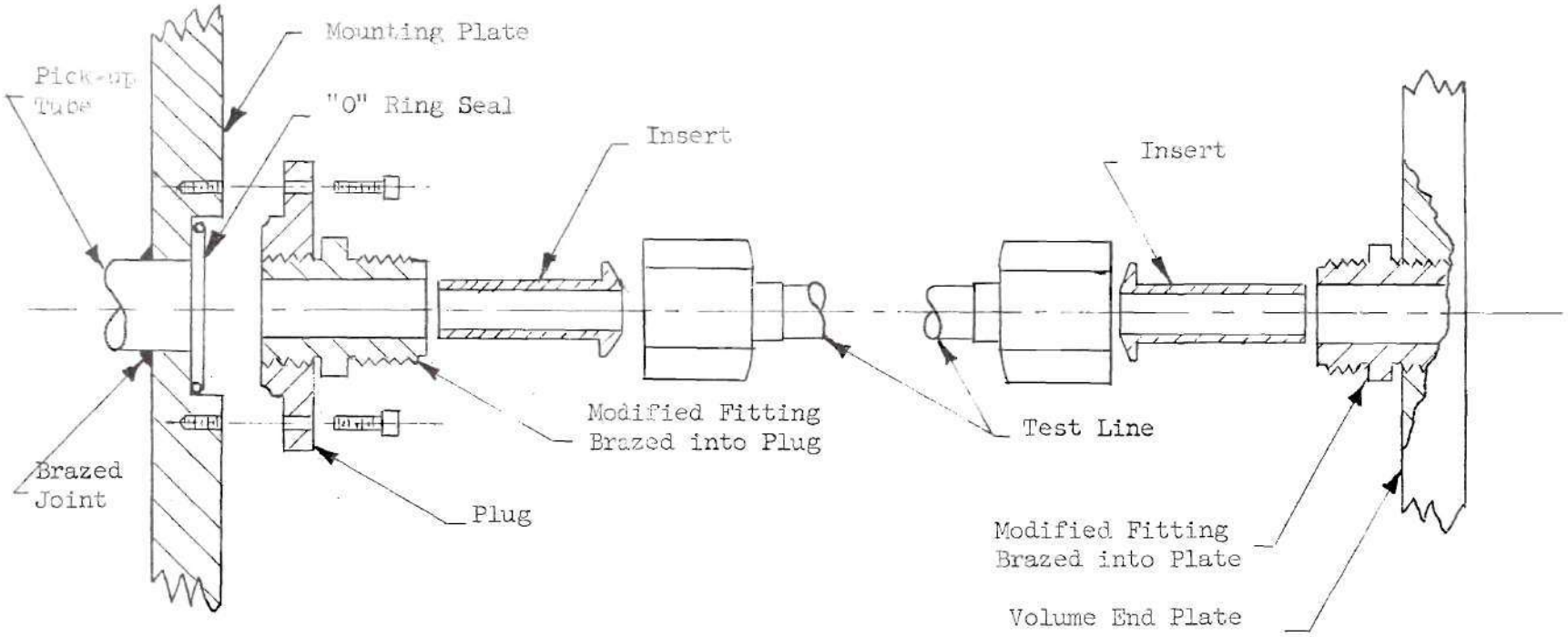

Fig. 5 Test Section Schematic

Figure 6). The pick-up tube was mounted so that its longitudinal axis could be aligned with the axis of symmetry of the shock tube nozzle. The longitudinal adjustment of the entrance of the pick-up tube was maintained at 1/8 inch inside the exit of the shock tube nozzle. The downstream end of the pick-up tube was connected to a modified tube fitting which held the upstream straight-through fitting for each diameter of test line used.

The test lines were standard, hard drawn steel tubes of various lengths and diameters (see Table 1). The ends of the tubes were flared at a 45° angle to connect to the modified tubing fittings on the pick-up tube and the receiver volume.

The straight-through fittings (Table 1) were machined from mild steel bar stock and one end of each fitting was beveled at a 45° angle to match the flares on the test lines. There were four sets of fittings for each of the two larger diameters of test line. No reduction fittings were used with the two smaller diameters of test line because the resulting inside diameters of the fittings are considerably smaller than those used in present pressure-sensing system designs.

Receiver Volume.--Three receiver volumes were tested. The smallest volume, 10.5 cubic inches, is shown in Figure 7. The other two volumes, 53.7 and 106.7 cubic inches, were similar to that shown in Figure 7 with the following exceptions: (1) the end plates were welded instead of bolted to the ends of the cylindrical pipe; (2) there were two different modified tube fittings in the upstream end of the volume. Two fittings were required to accommodate the various test line diameters and the fitting which was not in use was capped off. The 10.5 cubic inch volume

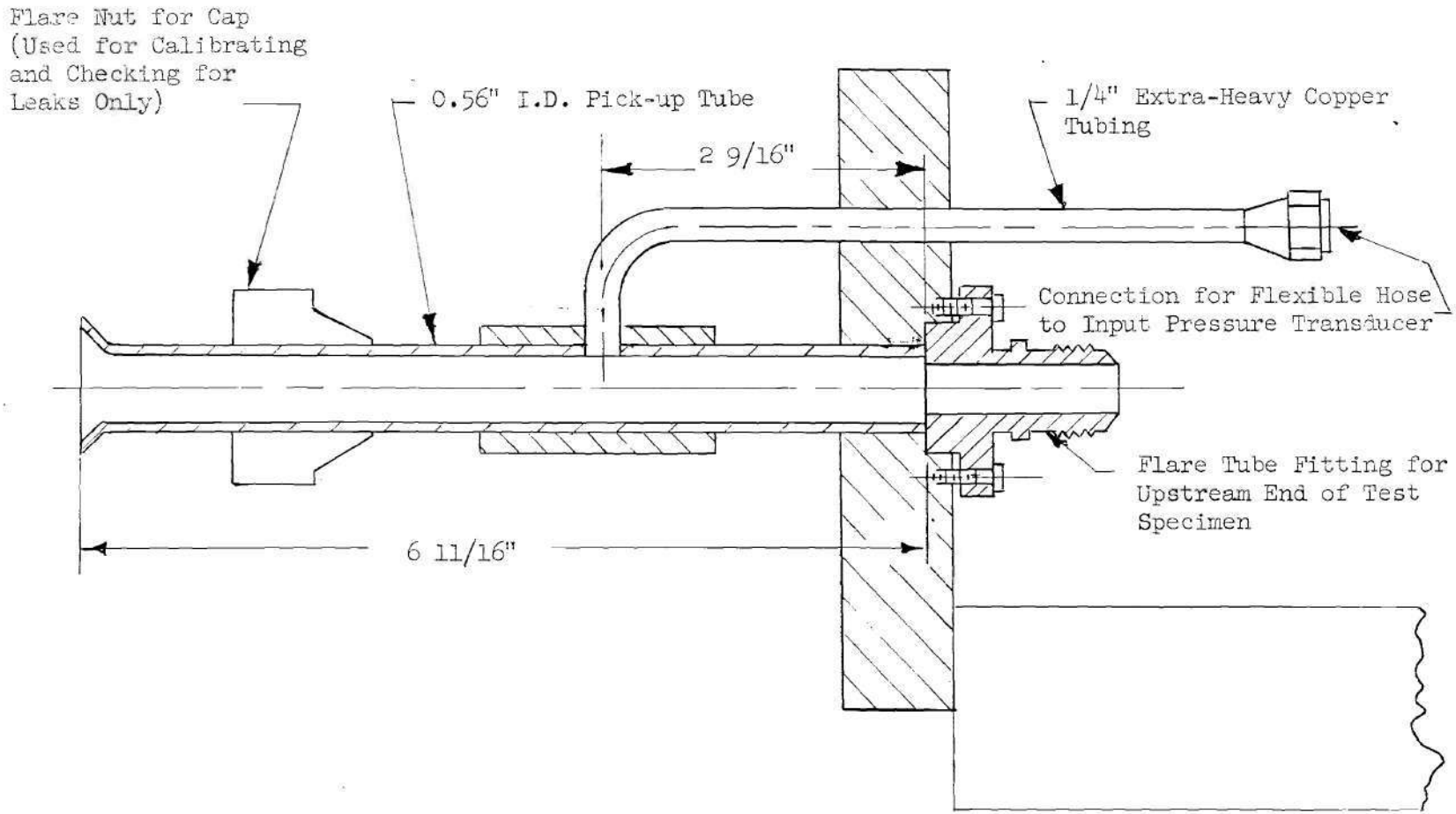

Fig. 6 Detail of Pick-up Tube

Table 1

Test Line and Reduction Insert Sizes*

Line diameter: 0.242 inches I.D.

Straight-Through Fitting I.D. (inches)	Diameter Ratio, %
0.242	100
0.220	89
0.170	69
0.121	50

Line diameter: 0.370 inches I.D.

Straight-Through Fitting I.D. (inches)	Diameter Ratio, %
0.370	100
0.332	88
0.242	62
0.190	51

Line diameter: 0.183 inches I.D.

Straight-Through Fitting I.D. (inches)

none

Line diameter: 0.114 inches I.D.

Straight-Through Fitting (inches)

none

* Line lengths of 1, 5, 10, and 15 feet were used for each line diameter.

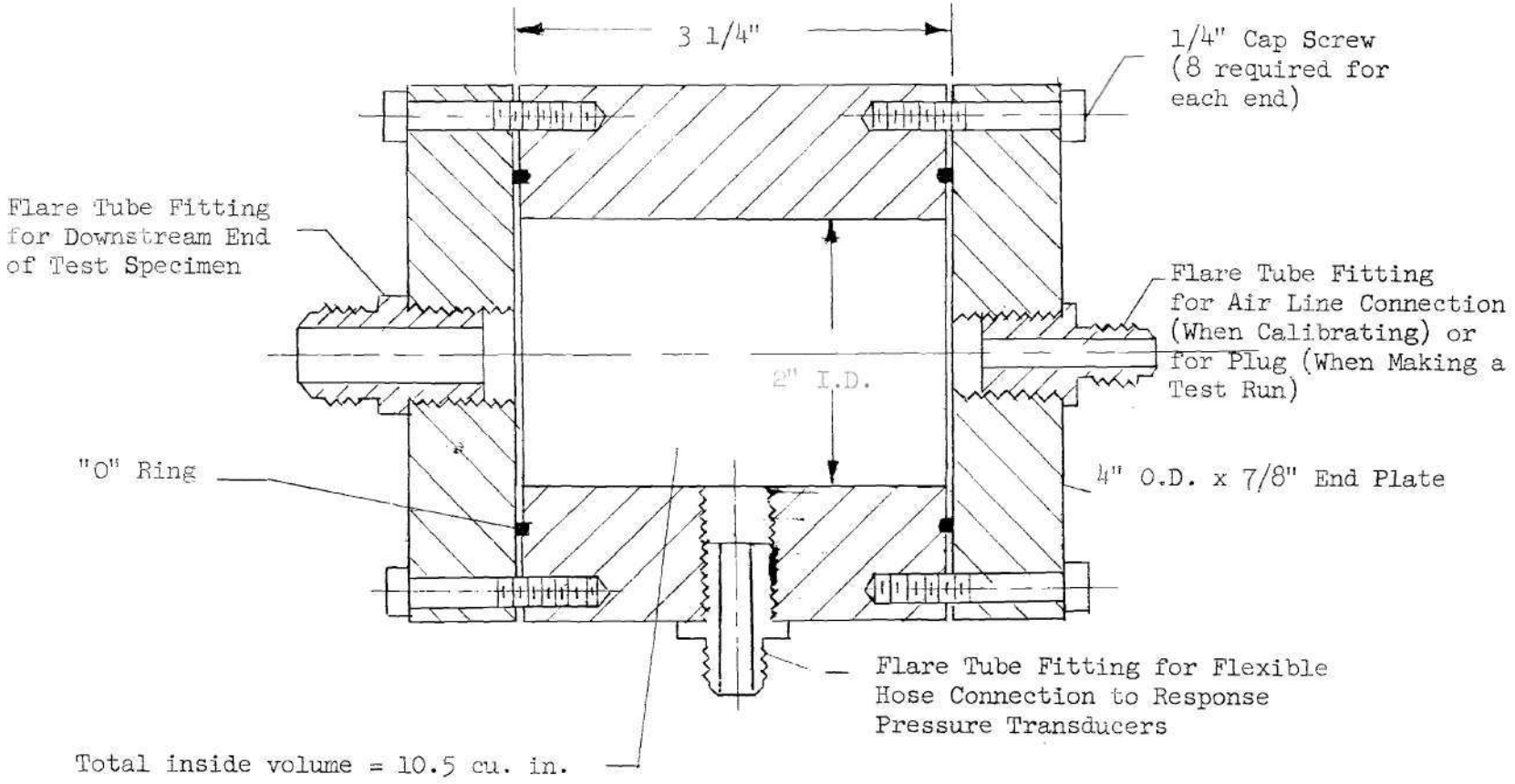

Fig. 7 Detail of Volume

had interchangeable end plates with different fittings to accommodate the various test line diameters.

Instrumentation.--The instrumentation consisted of two pressure-sensing transducers and data recording equipment.

A 0-1000 psig temperature compensated transducer was used to measure the input pressure at a point 4.2 inches downstream from the open end of the pick-up tube. A second transducer was used to measure the response pressure at a point midway between the end plates of the receiver volume. Two transducers were used interchangeably for this purpose to give reasonable sensitivity and accuracy. A 0-100 psig temperature compensated transducer was used to measure the response pressures below 100 psig and a 0-1000 psig temperature compensated transducer was used to measure the higher response pressures.

The 0-100 psig transducer was connected to the system with a 15 inch length of 3/8 inch I.D. flexible pressure hose via a 1/4 inch gate valve. The valve was closed to protect the transducer from the extreme over-pressures encountered when calibrating the 0-1000 psig input transducer and when checking the system for leaks.

Since pressures exceeding 1000 psig were never encountered in the test system, the 0-1000 psig input transducer and the 0-1000 psig response transducer, when used, were connected directly to the system with 15 inch lengths of flexible pressure hose.

The transducers were securely mounted in wooden saddle blocks and bolted to the concrete pad. The longitudinal axes of the transducers were placed normal to the direction of propagation of the external shock wave in order to minimize acceleration effects on the transducer output.

The electrical outputs from the transducers were linearly amplified through oscillator-powered carrier amplifiers and were recorded by an oscillograph. Fluid damped optical galvonometers in combination with the amplifiers gave the recording system a flat frequency response of 0-500 cycles per second. Light-sensitive paper was used in the oscillograph and was run at a speed of 42.8 inches per second. The oscillograph placed timing lines on the paper automatically at intervals of 0.01 seconds. The high paper speed was necessary in order to extend the record over a sufficient amount of paper to make the data reduction feasible and to increase the timing sensitivity.

Firing System.--The firing system consisted of a variable transformer, a firing switch, ohmmeter, connecting leads, firing element and diaphragm (see Figure 8).

The variable transformer was connected to a standard 115 volt AC power supply and was set for a voltage output of 16 volts AC.

The firing switch was a single pole, spring-loaded toggle switch. This type of switch was used so that the firing circuit could be closed only by the continuous application of pressure against the switch lever, thereby eliminating any possibility of the switch being left in the on position.

The ohmmeter was installed in parallel with the connecting leads to provide a constant check on the continuity and insulation of the firing element.

The connecting leads were two 15 foot lengths of standard, 14 gauge utility stranded electrical wire. A two-inch alligator clip was fastened to one end of each lead to provide a quick connection to the

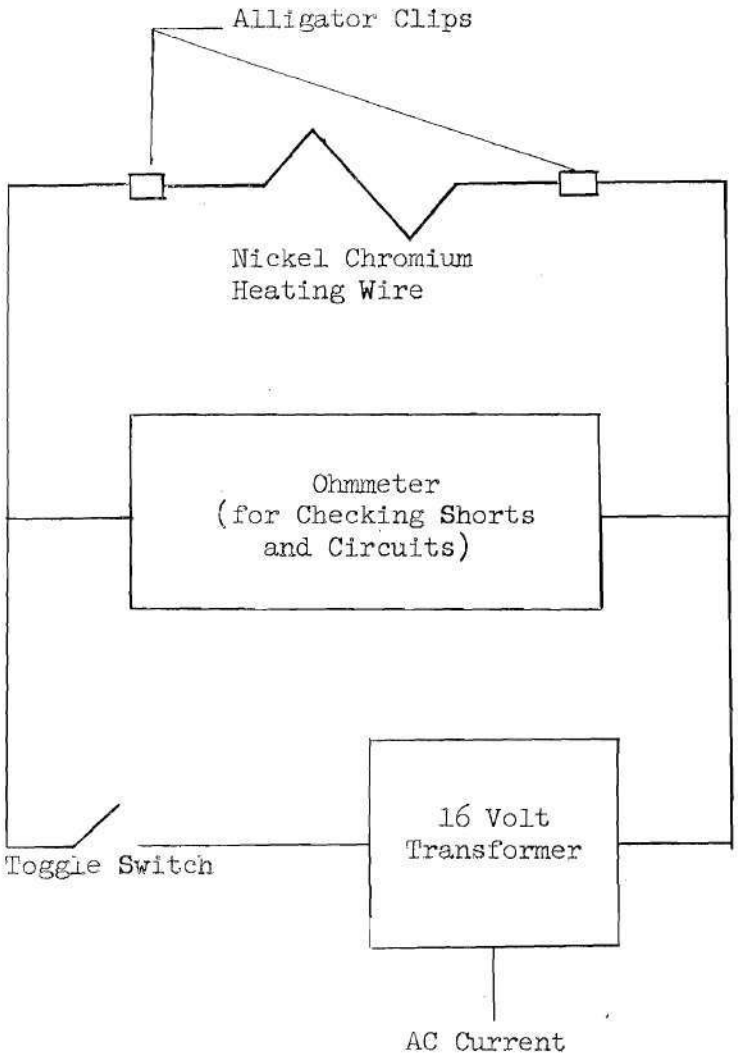

Fig. 8 Firing System

firing element.

The firing element was a 10-inch length of nichrome wire, 0.012 inches in diameter. The wire was bent in the form shown in Figure 9 and was placed between the layers of film in the diaphragm. The portions of the wire which passed between the shock tube and the nozzle were wrapped with tape to prevent any short circuits through the nozzle. The ends of the wire were formed into a loop to provide a good firm contact for the alligator clips on the connecting leads. A new wire was used with each diaphragm because continuous use of one wire caused the wire to become work-hardened and to break when the shock tube was pressurized and the diaphragm became distended.

The diaphragms were constructed from 3-inch circles of various thicknesses of polyester film. The thickness of each diaphragm depended on the shock tube pressure desired (see Table 2). The thickness of the diaphragms listed in Table 2 was sufficient to withstand the particular shock tube pressure, but allowed for rupture of the diaphragm with ease and reliability.

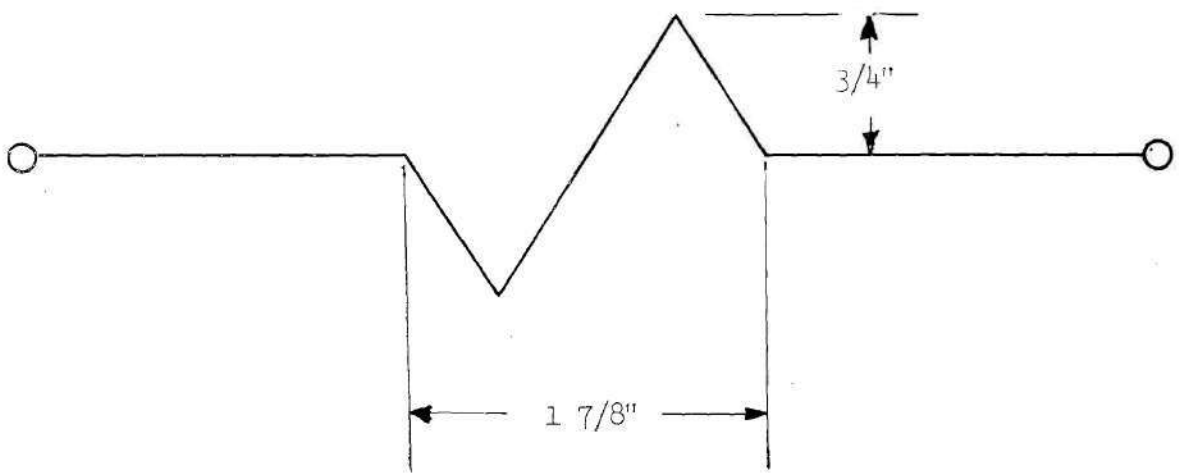

Fig. 9 Firing Element

Table 2

Diaphragm Thickness

Shock Tube Pressure (psig)	Diaphragm Thickness (inches)
50	0.0030
100	0.0060
200	0.0100
350	0.0150
500	0.0215
700	0.0300
1000	0.0450

* Diaphragms were constructed from polyester film.

CHAPTER III

PROCEDURE

All tests were performed outdoors at Research Area 2 of the Georgia Institute of Technology.

The experimental procedure used in testing each configuration consisted of:

1. obtaining a supply of high pressure air,
2. assembling the test configuration,
3. testing the configuration for leaks,
4. calibrating the transducers, and
5. firing the shock tube.

Air Supply.--After draining the four vapor separators on the compressor and the one on the control panel inlet, a quick maintenance check of the engine and compressor was made. The engine and compressor were started and the air storage tank was pressurized to 1200-1400 psig.

Test Configuration.--The desired test configuration, which consisted of a test line length and diameter, receiver volume and diameter reduction inserts in the straight-through fittings, was assembled. After sealing off the pick-up tube, the copper line used for calibration purposes was connected to the downstream face of the volume in preparation for leak testing.

Testing for Leaks.--The testing of the system for leaks consisted of pressurizing the test configuration in increments of 200 psig to a final pressure of 1000 psig. At each pressure level all joints, fittings and

connections of the configuration were checked with a mixture of soap and water. Also, the pressure sensitive gauge was watched for any noticeable decrease in pressure. When a leak was detected the system was bled down to atmospheric conditions and the source of trouble corrected. After all leaks were eliminated, provisions were made to begin calibration.

Calibration.--A calibration was made for each transducer at various amplifier attenuator settings. The necessity for different attenuator settings resulted from sensitivity requirements over the large range of input and response pressures investigated. Simultaneously with each pressure reading, a trace corresponding to the indicated pressure was recorded on the oscillograph. This trace was then measured from a reference line (atmospheric pressure) using a scale of sixty counts to the inch. Plots of calibration pressures versus counts were made for each attenuation setting. At least one calibration for each transducer and attenuation setting was made each day, along with occasional spot checks.

As suggested in Reference 3, a 1/4 inch diameter copper line with a needle valve was connected in such a manner as to bypass the small orifice that was used to protect the 1000 psig pressure gauge from damage due to a premature rupture of the diaphragm (see Figure 1). The valve was opened for calibration purposes and closed when operating the shock tube. This method saved considerable time during calibration by decreasing the length of time required for equilibrium to be attained in the gauge at each pressure level.

Firing Technique.--Preparations for the firing of the shock tube began with the placement of the diaphragm of the proper thickness (see Table

2) between the flange of the shock tube and the entrance of the nozzle. Sandwiched between the layers of the diaphragm was a nichrome heating wire formed as shown in Figure 9. After completion of the installation of the diaphragm, an ohmmeter was used to check the heating wire for short circuits between the wire and the shock tube or nozzle.

The alignment of the pick-up tube was checked to see that it was centered on the axis of the shock tube and 1/8 of an inch inside of the nozzle exit. Any necessary corrections were made by adjusting the recoil springs and guy wires on the table.

The two leads from the 16 volt AC firing circuit were attached to the nichrome heating wire and a final check of the circuit was made with the ohmmeter.

While the shock tube was being pressurized, the proper attenuation for each recording channel was set and the zero settings for each channel of the oscillograph were checked. After the system had come to equilibrium at the desired pressure, the inlet valve to the shock tube was closed. The oscillograph was started and the firing circuit was closed, causing the diaphragm to rupture. A series of runs, for each geometrical configuration, consisted of seven shock tube pressures: 50, 100, 200, 350, 500, 700, and 1000 psig.

CHAPTER IV

THEORY

The mathematical solution to the problem of transient flow in a simulated missile pressure sensing system is very difficult, due to the number of independent variables which must be considered: three spatial co-ordinated and time. Since the tubing and receiver volume are circular, the assumption of axial symmetry reduces the number of independent variables to three: radial and longitudinal co-ordinates and time. The problem can be simplified further by assuming the flow to be one-dimensional and by working with the average properties of the flow at any cross section along the longitudinal axis of the system. The assumption of one-dimensional flow reduces the problem to the consideration of only two independent variables: axial distance and time.

The mathematical solution to this simplified problem is still very difficult. The presence of two independent variables results in a partial differential equation which will be non-linear due to the non-linear effects of viscosity and compressibility.

The problem can be simplified further with the assumption that the mass flow past any section of the system is independent of the axial co-ordinate and dependent only upon time. This assumption of quasi-steady flow results in an uncoupling of the effects of the independent variables and the solution can be obtained from a non-linear ordinary differential equation.

The assumption of quasi-steady flow is very helpful in the problem under consideration, since the fundamental relations for steady flow can be integrated. The resulting equations are readily converted to quasi-steady flow by allowing the stream properties to be functions of time. Also, the quasi-steady flow assumption suggests the possibility of using data obtained from steady flow experiments to aid in the development of the theory.

Steady One-Dimensional Flow In A Circular Tube.--Consider the steady flow of a gas through a long circular tube of constant cross-sectional area, based on the following assumptions:

(1) The flow is isothermal

(2) The pressure p, density ρ, and temperature T satisfy an equation of state of the form

$$p = \rho RT \tag{4-1}$$

where R is a gas constant.

The isothermal assumption is made in order to develop a theory which can be applied to the simulated pressure-sensing system. In such systems, for the present pressure input functions, the isothermal assumption is difficult to justify. However, it is felt that most of the time for a given run, i.e., after the shock wave has entered the sensing volume, the flow rate is at a low enough level so that the assumption of isothermal flow is probably valid.

For steady flow through a tube with constant cross-sectional area (Figure 10), the continuity equation can be written as

$$\frac{W}{A} = \rho U = G \text{ , a constant} \tag{4-2}$$

where

w is the rate of mass flow through the tube

A is the cross-sectional area of the tube

ρ is the density of the gas

U is the mean velocity of the gas passing any section.

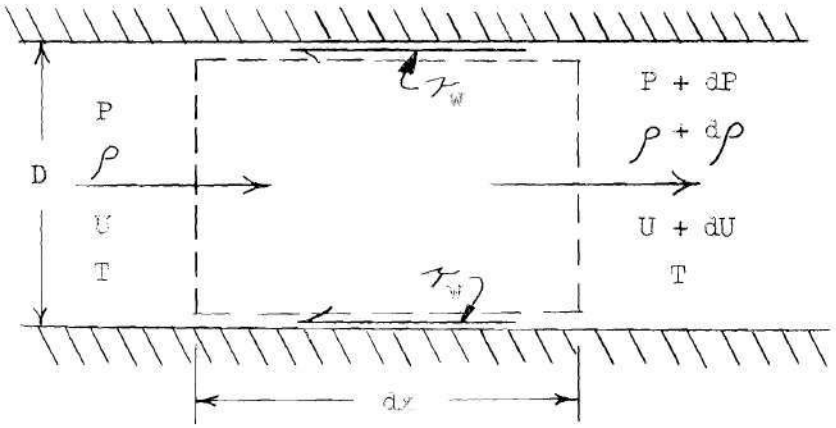

Fig. 10 Control Volume for Analysis of Steady, One-Dimensional Isothermal Flow

Referring to Figure 10, the momentum equation can be written

$$pA - (p + dp)\,A - \tau_w \frac{4A}{D}\,dx = w\,dU$$

or

$$A\,dp + \tau_w \frac{4A}{D}\,dx + w\,dU = 0 \qquad (4\text{-}3)$$

where

τ_w is the wall shearing stress

$\frac{4A}{D}\,dx$ is the wetted wall area over which the wall stress acts

A is the cross-sectional area of the tube

D is the diameter of the tube.

The local friction factor is defined by

$$f = \frac{\tau_w}{1/2 \rho U^2} \tag{4-4}$$

Substitution of Equation (4-4) into Equation (4-3) and multiplication by P/A yields,

$$\rho dp + 1/2(\rho U)^2 \frac{4f}{D} dx + \frac{W}{A}(\rho U) \frac{dU}{U} = 0 \tag{4-5}$$

Substitution into Equation (4-5) for ρ from Equation (4-1) and for ρU from Equation (4-2) yields,

$$\frac{pdp}{RT} + 1/2\left(\frac{W}{A}\right)^2 \frac{4fdx}{D} + \left(\frac{W}{A}\right)^2 \frac{dU}{U} = 0 \tag{4-6}$$

Now, differentiation of Equations (4-1) and (4-2) yields, for isothermal flow,

$$\frac{dU}{U} = -\frac{d\rho}{\rho} = -\frac{dp}{p} \tag{4-7}$$

Substitution of Equation (4-7) into Equation (4-6) and simplifying gives,

$$\frac{2pdp}{RT} + \left(\frac{W}{A}\right)^2 \left[\frac{4fdx}{D} - 2\frac{dp}{p}\right] = 0 \tag{4-8}$$

Under the assumption of isothermal flow, Equation (4-8) can be integrated between sections I and II as follows:

$$\frac{1}{RT}\int_{I}^{II} 2p\,dp + \left(\frac{W}{A}\right)^2\left[\int_{I}^{II}\frac{4f}{D}\,dx - 2\int_{I}^{II}\frac{dp}{p}\right] = 0$$

or

$$\frac{P_{II}^2 - P_I^2}{RT} + \left(\frac{W}{A}\right)^2\left[\frac{4\bar{f}L}{D} - 2\ln\frac{P_{II}}{P_I}\right] = 0 \qquad (4\text{-}9)$$

where

$$\bar{f} = \frac{1}{L}\int_{I}^{II} f\,dx \qquad (4\text{-}10)$$

and

$$L = X_{II} - X_I$$

Equation (4-10) represents a mean friction factor $\bar{f}$; however, it should be noted that in this case $\bar{f}$ also contains development losses since the integration of Equation (4-8) has been performed over the entire length of the tube.

Also, it should be noted that the integration of Equation (4-8) is equally valid for quasi-steady flow.

Equation (4-9) can be solved explicitly for W^2 as follows

$$W^2 = \frac{A^2}{RT}\left[\frac{P_I^2 - P_{II}^2}{\frac{4\bar{f}L}{D} + 2\ln\left(\frac{P_I}{P_{II}}\right)}\right] \qquad (4\text{-}11)$$

Empirical Application To A More Complicated Geometry.--The immediate application of Equation (4-11) is to systems of the type shown in Figure 11, where the pressures P_1 and P_2 are now measured in the entrance and exit pipes respectively, rather than in the test tube itself.

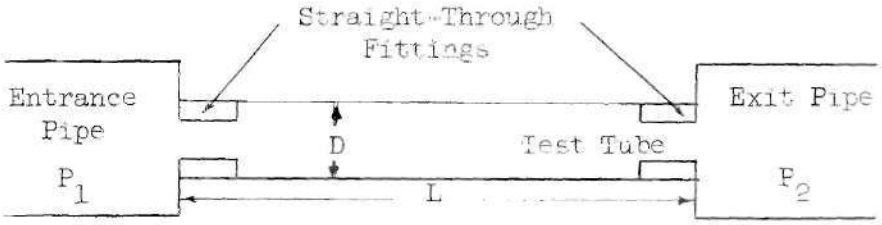

Fig. 11 Schematic of Typical Flow System

Flow through this system differs from considered in the development of Equation (4-11) in the following respects:

(i) Losses occur in the entrance to the test-tubing and in the sudden expansion at the exit from the test tubing.

(ii) Addition losses occur if the inside diameter of the fittings is smaller than the inside diameter of the tube.

(iii) As previously mentioned, the pressures P_1 and P_2 are not measured in the test tube.

It would be convenient if these losses could be combined along with the friction and development losses into a "pseudo friction factor" which would be similar to the friction factor of ordinary engineering practice. Define such a "pseudo friction factor", f^*, by the relation

$$w^2 = \frac{A^2}{RT}\left[\frac{P_1^2 - P_2^2}{4f^* \frac{L}{D}}\right] \qquad (4\text{-}12)$$

Comparison of Equation (4-12) with Equation (4-11) shows that f^* incorporates development losses, entrance and exit losses, and compressibility losses along with friction losses for the fully-developed portion of the flow.

References 4, 5 and 6 have shown that the experimental data for f^* from steady flow experiments can be fitted approximately by equations of the type

$$f^* = \frac{C}{Rey^N} \qquad (4\text{-}13)$$

where

C is a constant.

Rey is the pipe Reynolds number.

N is an exponent whose value depends on whether the flow is laminar or turbulent.

C and N also depend upon the fitting diameter ratio a.

Now, the Reynolds number is coupled to the mass flow through the relation

$$Rey = \frac{\rho V D}{\mu} = \frac{w}{A}\frac{D}{\mu} \qquad (4\text{-}14)$$

where

μ is the coefficient of viscosity.

Substitution of Equation (4-14) into Equation (4-13) yields

$$f^* = C\left[\frac{A\mu}{wD}\right]^N \qquad (4\text{-}15)$$

Substitution of Equation (4-15) into Equation (4-12) gives

$$w^2 = \frac{A^2}{RT}\left[\frac{P_1^2 - P_2^2}{\frac{4C}{w^N}\left(\frac{\Delta\mu}{D}\right)^N \frac{L}{D}}\right]$$

or, solving for w

$$w^{2-N} = \frac{A^2}{RT}\left[\frac{P_1^2 - P_2^2}{4C\left(\frac{\Delta\mu}{D}\right)^N \frac{L}{D}}\right]$$

or,

$$w = \frac{\pi}{4}\left[\frac{D^{3-N}}{4CR\Delta\mu^N L}\right]^{\frac{1}{2-N}}\left[P_1^2 - P_2^2\right]^{\frac{1}{2-N}} \qquad (4\text{-}16)$$

Equation (4-16) is the equation for the steady state mass rate of flow through a tube, where the pressures P_1 and P_2 are measured in the entrance and exit pipes, respectively, and the constants C and N are determined from steady state experiments. It should be noted that Equation (4-16) is also assumed to be applicable for quasi-steady flow, where P_1 and P_2 are functions of time.

CHAPTER V

TRANSIENT FLOW IN PRESSURE SENSING SYSTEMS

Theory.--One type of static pressure sensing system suitable for use in missiles consists essentially of a length of tubing connecting a static pressure tap, on the surface of the missile, with a pressure measuring instrument having an internal volume (Figure 12).

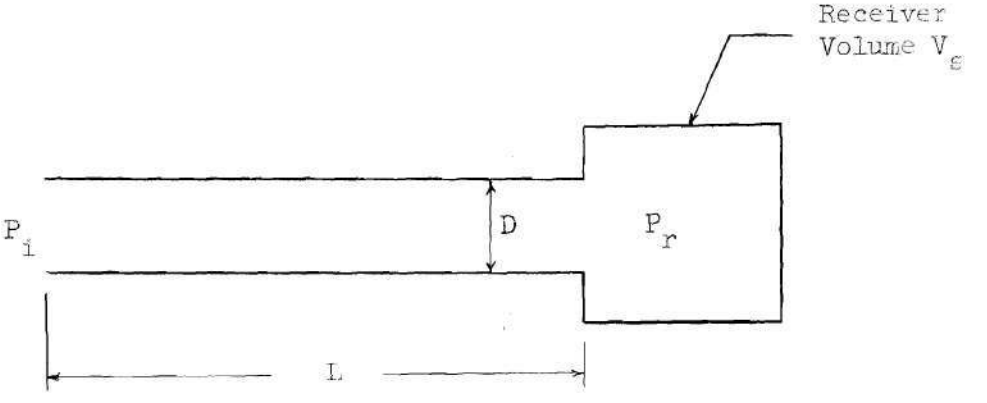

Fig. 12 Schematic of Simulated Missile Pressure Sensing System

The theory developed in Chapter IV may be applied to a time-dependent flow in this type of system if the flow is assumed to be quasi-steady. For a quasi-steady flow, the mass flow in the system (which is a function of time only) is assumed to be given by Equation (4-17).

Thus,

$$w = w(t) = \frac{\pi}{4}\left[\frac{D^{5-N}}{4CRT\mu^{N}L}\right]^{\frac{1}{2-N}}\left[P_1^2(t) - P_2^2(t)\right]^{\frac{1}{2-N}} \qquad (5\text{-}1)$$

where

$P_1(t)$ is the input pressure P_i and

$P_2(t)$ is the response pressure P_r .

The equation of state for the gas in the system can be written as

$$\bar{p}V = mRT \qquad (5\text{-}2)$$

where

V is the total volume of the system

m is the mass of air in the system

T is the absolute temperature of the gas in the system

$\bar{p}$ is the mean pressure in the system given by

$$\bar{p} = \frac{1}{V}\int_V p\,dV$$

Again assuming isothermal flow, Equation (5-2) can be differentiated with respect to time to give the mass rate of flow at the entrance to the tube as

$$w = \frac{dm}{dt} = \frac{V}{RT}\frac{d\bar{p}}{dt} \qquad (5\text{-}3)$$

For the systems under consideration, the sensing volume is always greater than the internal volume of the tubing; hence the mean pressure is weighted toward the response pressure. Thus, it is assumed that

little error is introduced by replacing the derivative of the mean pressure by the derivative of the response pressure, that is

$$\frac{d\bar{p}}{dt} \quad \frac{dP_r}{dt} \tag{5-4}$$

Substitution of Equation (5-4) into Equation (5-3) gives

$$w = \frac{V}{RT}\frac{dP_r}{dt} \tag{5-5}$$

Elimination of w between Equations (5-1) and (5-5) gives

$$\frac{V}{RT}\frac{dP_r}{dt} = \frac{\pi}{4}\left[\frac{D^{5-N}}{4CRT\mu^N L}\right]^{\frac{1}{2-N}} \left[P_i^2(t) - P_r^2(t)\right]^{\frac{1}{2-N}}$$

or simplifying

$$\frac{dP_r}{dt} = \frac{\pi}{4}\frac{(RT)^{\frac{1-N}{2-N}}}{(C\mu^N)^{\frac{1}{2-N}}}\frac{D^{\frac{5-N}{2-N}}}{L^{\frac{1}{2-N}}\cdot V}\left[P_i^2(t) - P_r^2(t)\right]^{\frac{1}{2-N}} \tag{5-6}$$

Equation (5-6) is the general form of the differential equation for the response pressure, P_r, of the system to an input pressure, P_i. Since Equation (5-6) was developed on the assumption of quasi-steady flow, the steady flow experiments (References 4, 5 and 6) are assumed to be applicable for the evaluation of the constants C and N for the two flow regimes, laminar and turbulent.

Laminar Flow.--The development of the theory for laminar flow is presented purely for demonstration purposes and will not be used in this investigation. For fully-developed steady flow in circular tubes theory

and experiments (Reference 7) are correlated by the relation

$$4\bar{f} = \frac{64}{Rey} \tag{5-7}$$

Steady flow experiments (References 4, 5 and 6) indicate that for Reynolds numbers less than 100 the difference between $\bar{f}$ and f^* is negligible for tubes with or without reduction fittings. Thus, for this range of Reynolds numbers, substitution of

$$C = 64$$

$$N = 1$$

into Equation (5-6) yields

$$\frac{dP_r}{dt} = \frac{\pi}{256\mu} \frac{D^4}{LV} \left[P_i^2(t) - P_r^2(t)\right] \tag{5-8}$$

Equation (5-8) is the differential equation for laminar flow with Reynolds numbers less than 100. For convenience in the evaluation of experimental data, a system geometry parameter ϕ is defined by

$$\phi = \frac{10^4 D^4}{L V} \tag{5-9}$$

where the factor of 10^4 is introduced for numerical convenience only.

Now Equation (5-8) is written as

$$\frac{dP_r}{dt} = K \left[P_i^2(t) - P_r^2(t)\right] \tag{5-10}$$

where

$$K = \frac{\pi \phi}{256\mu(10)^4} \tag{5-11}$$

The application of Equation (5-10) is illustrated in Reference 8.

Turbulent Flow.--From the data obtained from References 4, 5 and 6, it was determined that for turbulent flow through a tube with no reduction fittings

$$f^* \quad \frac{0.085}{Rey^{0.1}} \tag{5-12}$$

Substitution of

$$C = 0.085$$

$$N = 0.1$$

into Equation (5-6) yields

$$\frac{dP_r}{dt} = 2.874 \left[\frac{R^9 T^9}{\mu}\right]^{0.5263} \frac{D^{2.5789}}{L^{0.5263} V} \left[P_i^2(t) - P_r^2(t)\right]^{0.5263} \tag{5-13}$$

Equation (5-13) is the response pressure differential for turbulent flow through a tube with no reduction fittings. Again, for convenience in evaluating the experimental data, a system geometry parameter, ψ, is defined by

$$\psi = \frac{(100D)^{2.5789}}{L^{0.5263} V} \tag{5-14}$$

where the factor $(100)^{2.5789}$ is introduced for numerical convenience only. Now, Equation (5-13) can be written as

$$\frac{dP_r}{dt} = M \left[P_i^2(t) - P_r^2(t) \right]^{0.5263} \qquad (5\text{-}15)$$

where

$$M = 1.998(10^{-5}) \left[\frac{R^9 T^9}{\mu} \right]^{0.5263} \qquad (5\text{-}16)$$

CHAPTER VI

DISCUSSION OF RESULTS

The results of this investigation are restricted to tube lengths from one to 15 feet, tube diameters from 0.114 to 0.370 inches, receiver volumes from 10.5 to 106.7 cubic inches and straight-through fittings with inside diameters of 50 to 100 per cent of the tubing diameters. The results are further restricted to shock-type inputs with strengths between 30 and 700 psig and to ambient flow temperatures in the range of 520 to 540 degrees Rankine.

A typical experimental run, shown in Figure 13, illustrates several aspects of the experimental results. It is believed that the rapid fluctuations in the input pressure curve are due to reflected pressure waves inside the system and to mechanical vibrations of the system itself.

From the experimental data, plots of maximum response pressure, $P_{r_{max}}$, versus maximum input pressure, $P_{i_{max}}$, were made for each geometric configuration. A representative curve illustrating the variation of $P_{r_{max}}$ with $P_{i_{max}}$ is shown in Figure 14. These plots indicate that $P_{r_{max}}$ is approximately linear with $P_{i_{max}}$ which is in agreement with the results of Reference 3.

The qualitative variations of the attenuation of the shock waves with the system geometric dimensions are shown in Figures 15, 16, 17 and 18 wherein the effects of length, diameter, volume, and straight-through

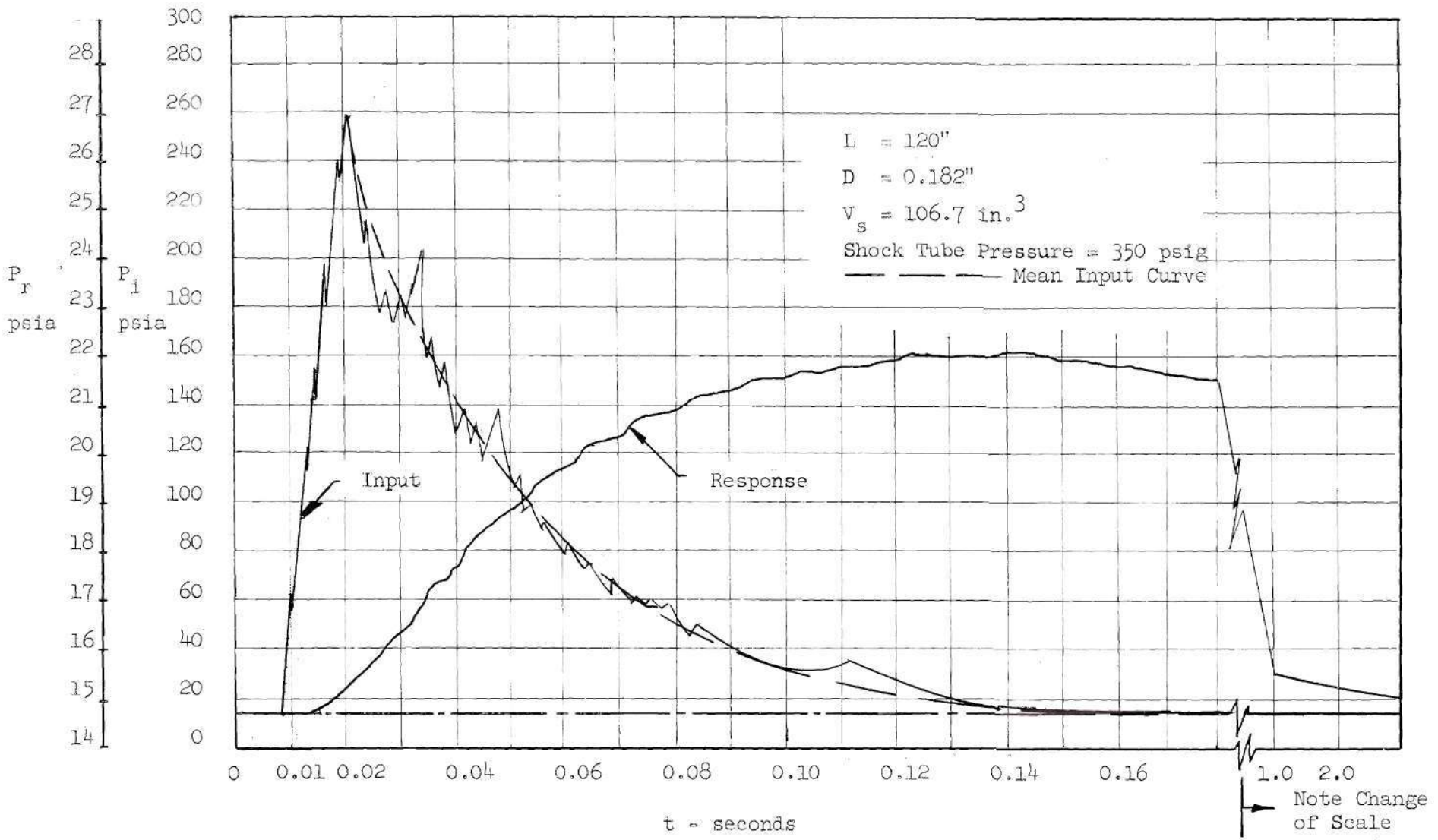

Fig. 13 Typical Test Run

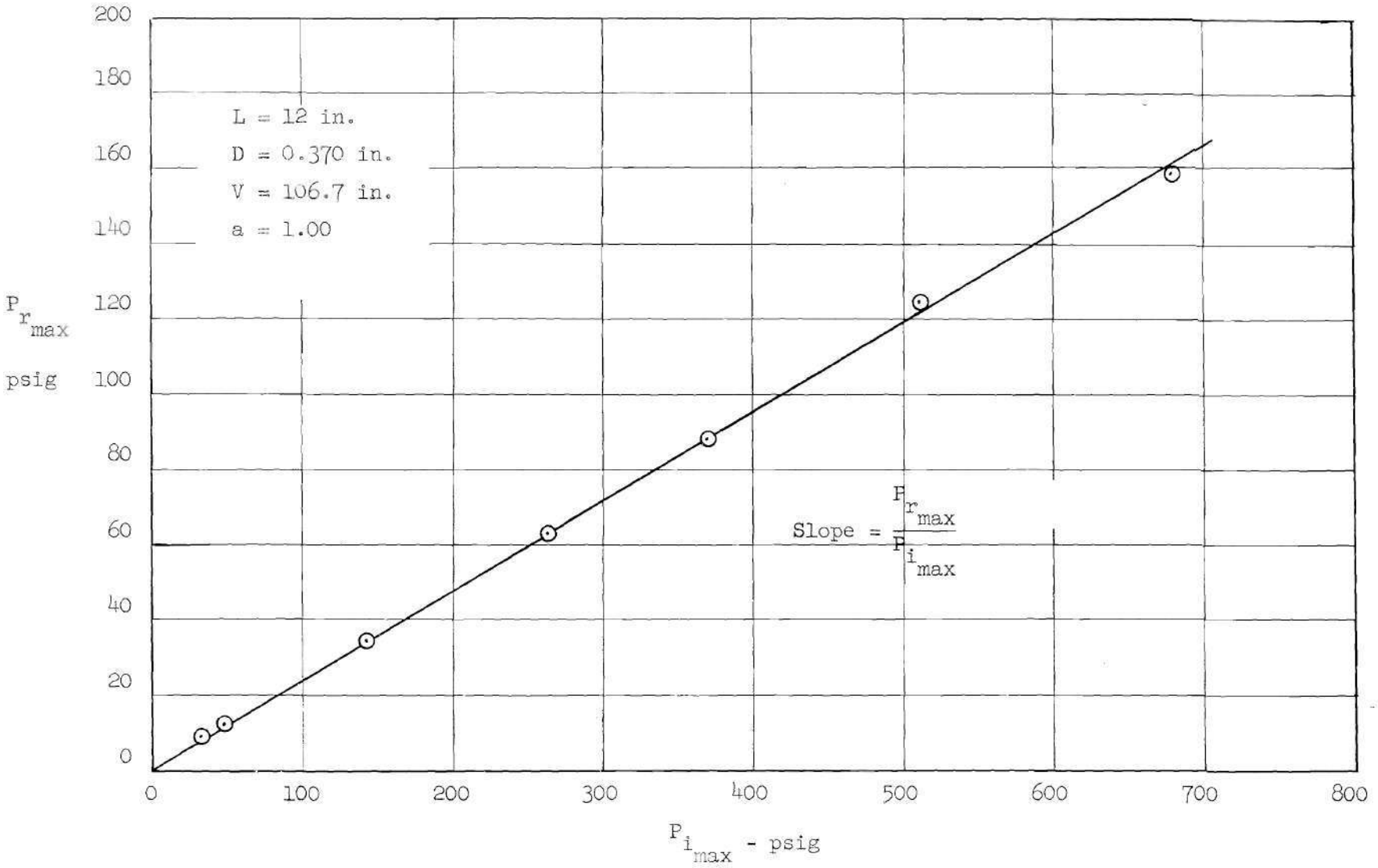

Fig. 14 Maximum Response Pressure Versus Maximum Input Pressure for a Typical System

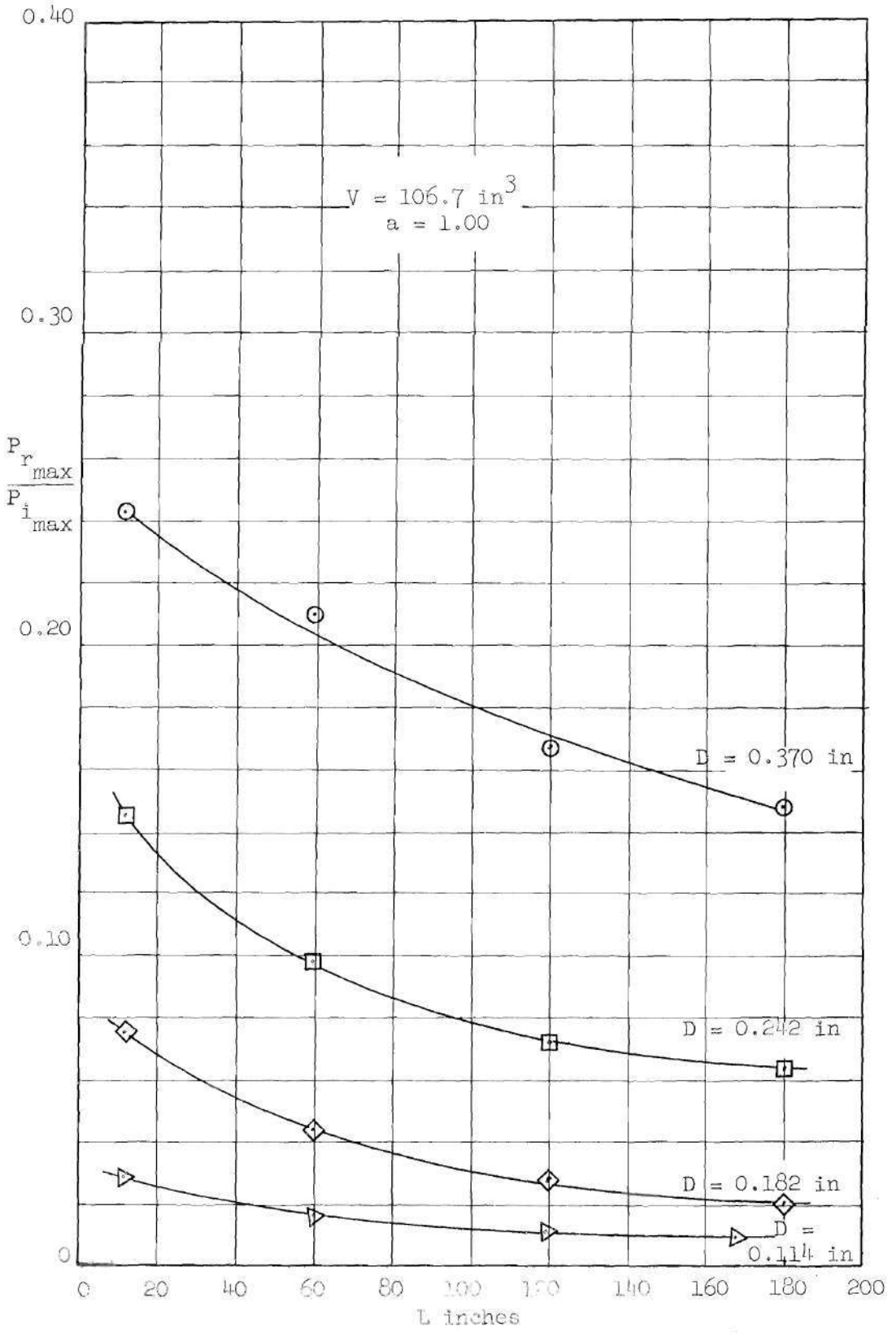

Fig. 15 Effect of Length on Shock Wave Attenuation

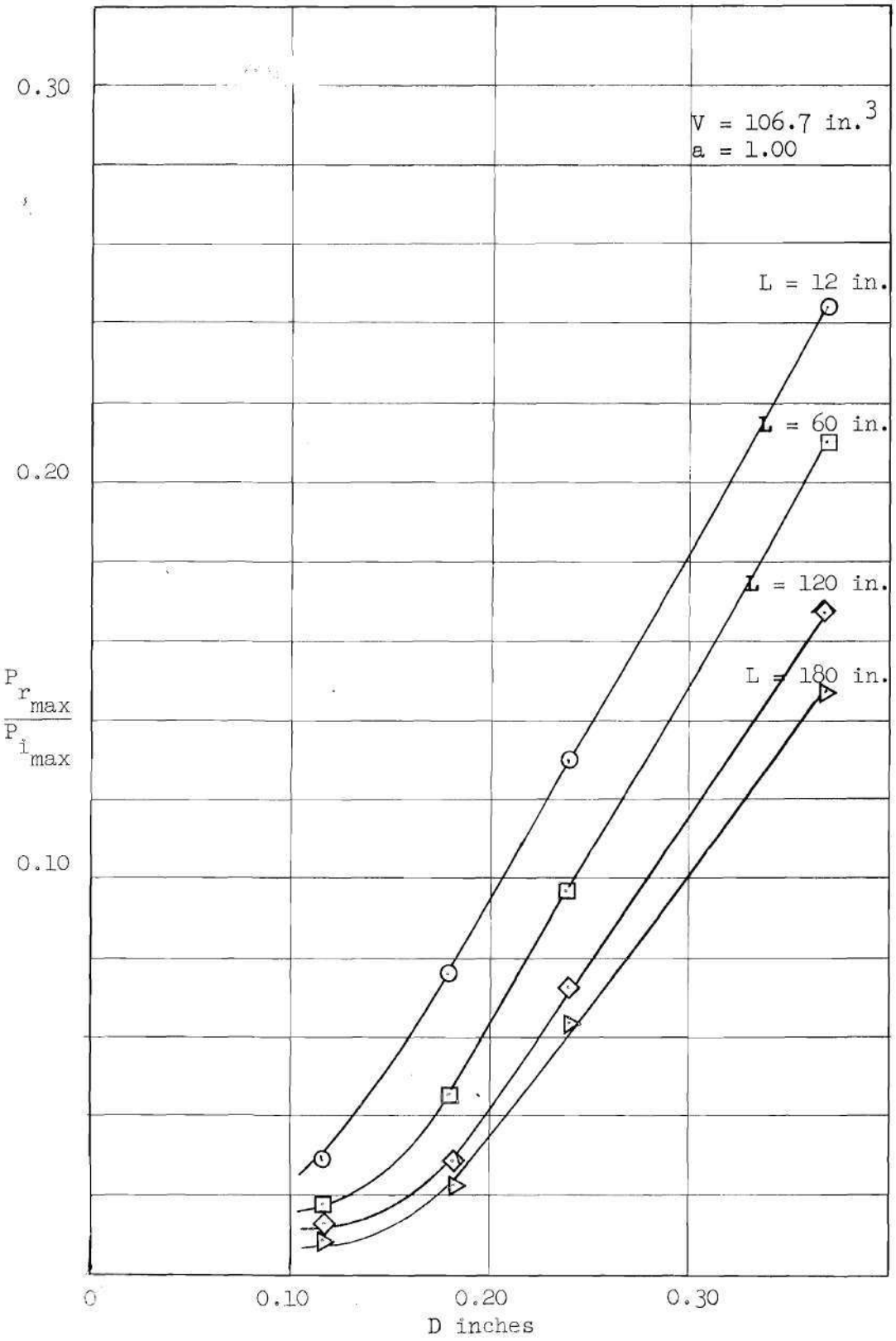

Fig. 16 Effect of Diameter on Shock Wave Attenuation

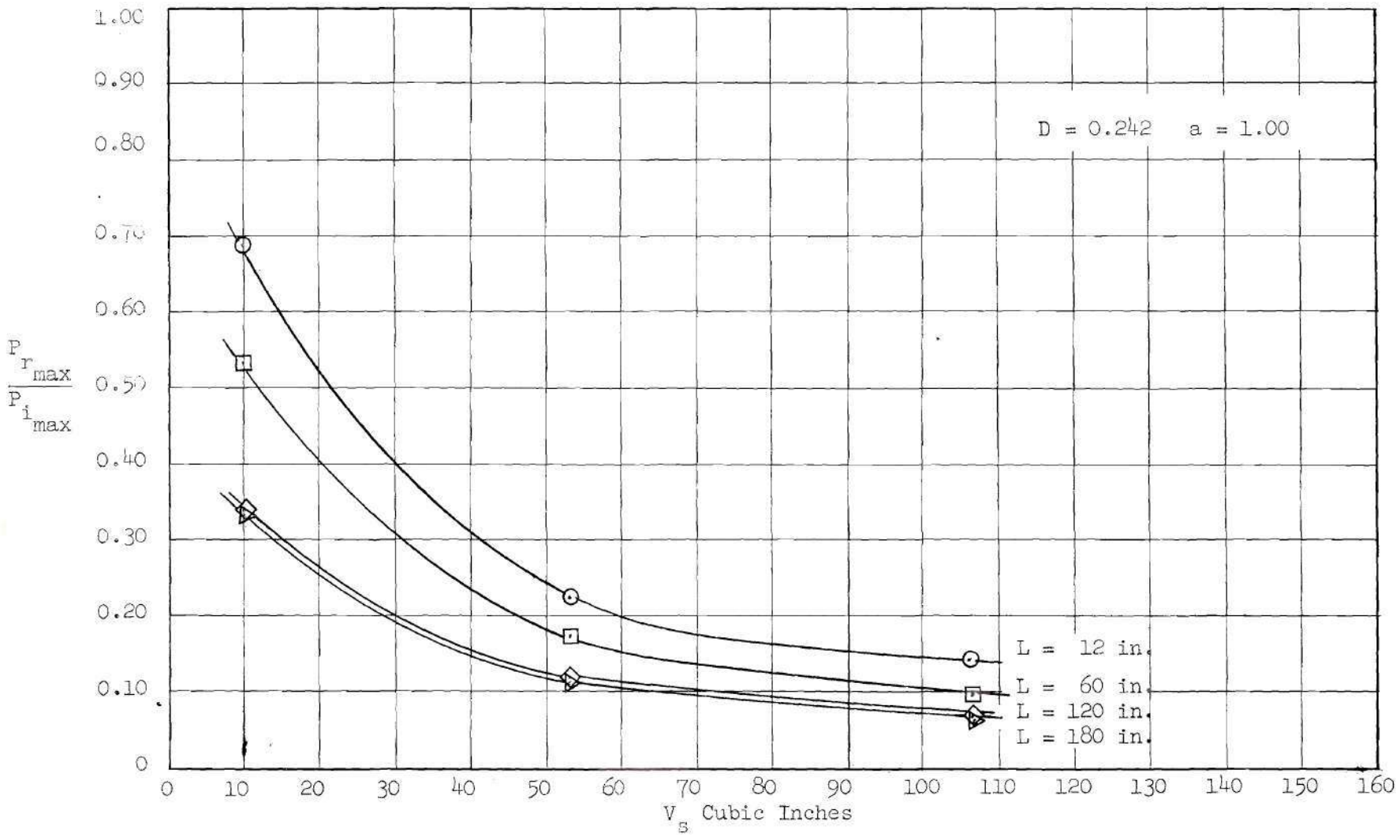

Fig. 17 Effect of Receiver Volume on Shock Wave Attenuation

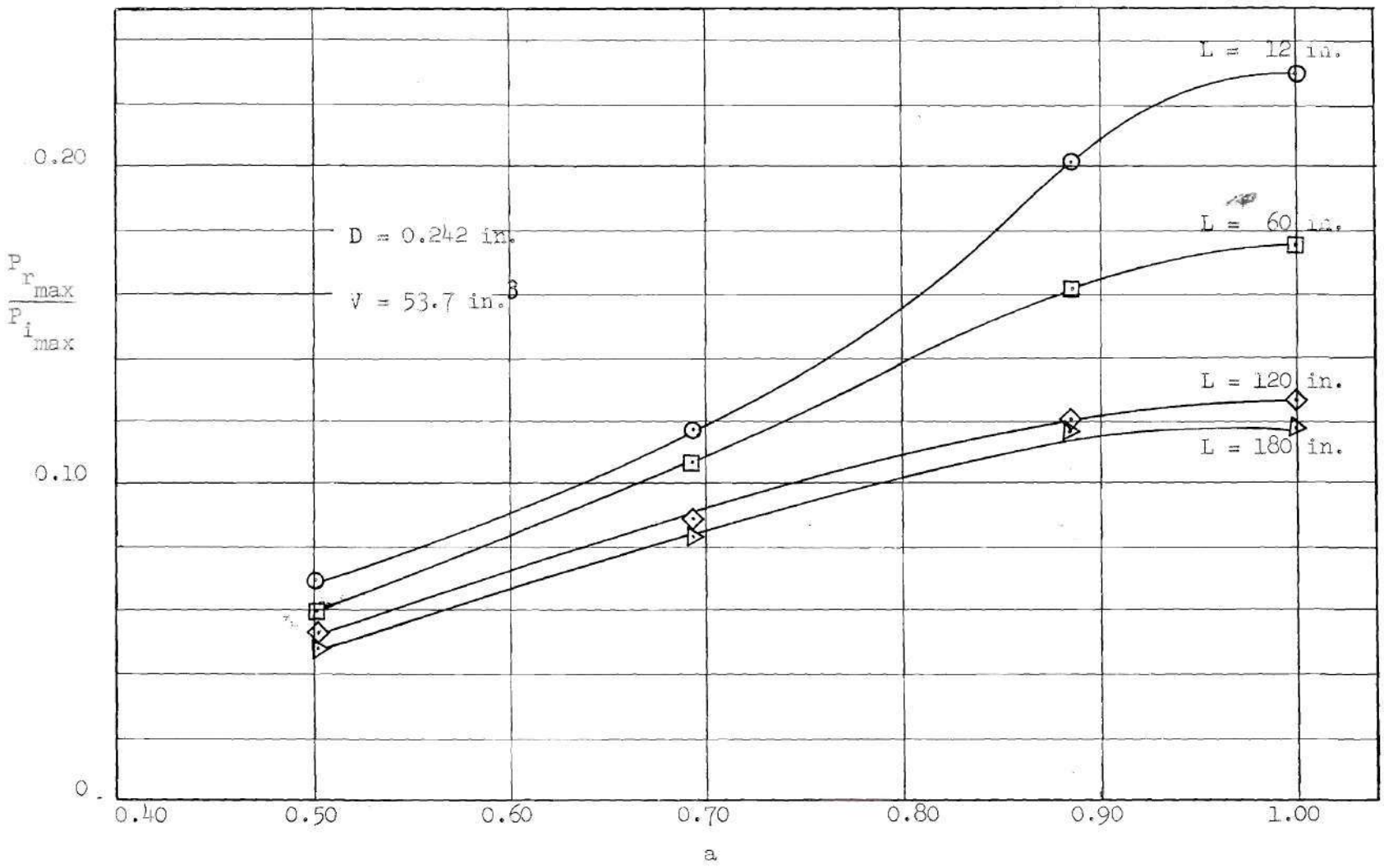

Fig. 18 Effect of Straight-Through Fittings on Shock Wave Attenuation

fittings are shown, respectively.

Correlation Of The Semi-Empirical Theory With Experiment.--Before the semi-empirical theory can be applied to any problem, the type of flow which exists in the tubing (i.e. laminar or turbulent) must be determined. A qualitative indication of the type of flow which results from a particular input function can be determined as follows: with the known input pressure function, calculate the mass flow in the tube at time $t = 0^+$ (where the response pressure has risen only slightly and can be taken as being equal to the initial response pressure) for laminar flow and turbulent flow using Equations (5-10) and (5-15). When the mass flows are known, the corresponding Reynolds numbers can be calculated from Equation (4-14).

$$Rey = \frac{w}{A}\frac{D}{\mu} \qquad (4\text{-}14)$$

A comparison of the resulting Reynolds numbers with the experimental data from Reference 6 (for the transition Reynolds number of flow in hard drawn steel tubes with sharp-edged entrance conditions and straight-through reduction fittings) will give a qualitative indication of which type of flow exists for a particular input pressure function.

When the type of flow (laminar or turbulent) has been determined, the appropriate equation (Equation 5-10 or 5-15) can be used to determine the response pressure as a function of time for a known input pressure function. It should be noted that the theory can also be applied to a response pressure function in order to calculate the input function.

The experimental data indicated that the shock-type pressure inputs resulted in a turbulent flow. However, it is felt that a small

transition region and a small laminar flow region must exist as the response pressure returns to atmospheric pressure at the end of each run. Since the semi-empirical theory does not apply to a transition region, the shock-type input pressures were assumed to cause a completely turbulent flow and Equation (5-15) was used for the complete run.

Equation (5-15) was integrated numerically for several test configurations incorporating straight-through fittings with inside diameters equal to those of the test tubes. The configurations selected for the integration were such that they covered the range of the geometric parameter, Ψ , given by Equation (5-14).

The integration was carried out by means of a "predictor-corrector" method using the following four equations:

$$P_r'(t) = M\left[P_i^2(t) - P_r^2(t)\right]^{0.5263} \tag{5-15}$$

$$P_{r_1}(t + \Delta t) = P_r(t) + P_r'(t)\,\Delta t \tag{6-1}$$

$$P_r'(t + \Delta t) = M\left[P_i^2(t + \Delta t) - P_{r_1}^2(t + \Delta t)\right]^{0.5263} \tag{6-2}$$

$$P_{r_2}(t + \Delta t) = P_r(t) + \frac{\Delta t}{2}\left[P_r'(t) + P_r'(t + \Delta t)\right] \tag{6-3}$$

where subscripts 1 and 2 denote successive approximations to P_r and Δt is a suitably chosen time interval.

Two input strengths were used in several cases to check the theory for both high and low strength shock waves.

Since the rapid fluctuations in the input pressure are very difficult to handle in Equation (5-15), an average curve was faired through the input function as shown by the dashed line in Figure 13.

Equation (5-15) was then integrated several times for each particular average input function and geometric configuration using different values of the parameter M until reasonable correlation between theory and experiment for the transient response pressure was realized. The results of the numerical integrations are compared with experiment in Figures 19-23.

A comparison is made in Figure 24 between the values of M obtained from integration of Equation (5-15) and the values of M predicted by Equation (5-16). The agreement in the comparison is seen to be reasonable. The scattering of the values of M obtained by integrating Equation (5-14) probably results from two reasons:

(1) the experimental runs were of such short duration (in some instances less than 0.25 seconds) that accurate measurements of the flow temperature could not be made, and

(2) the very rapid increase in the input pressure at the beginning of the run (Figure 13) made data reduction in this region difficult, thus the input pressure functions used in Equation (5-15) were probably in error in this region.

Any error in the input pressure function is propagated in the direction of integration. However, it is believed that the use of steady-state data to predict the character of the flow equation in conjunction with

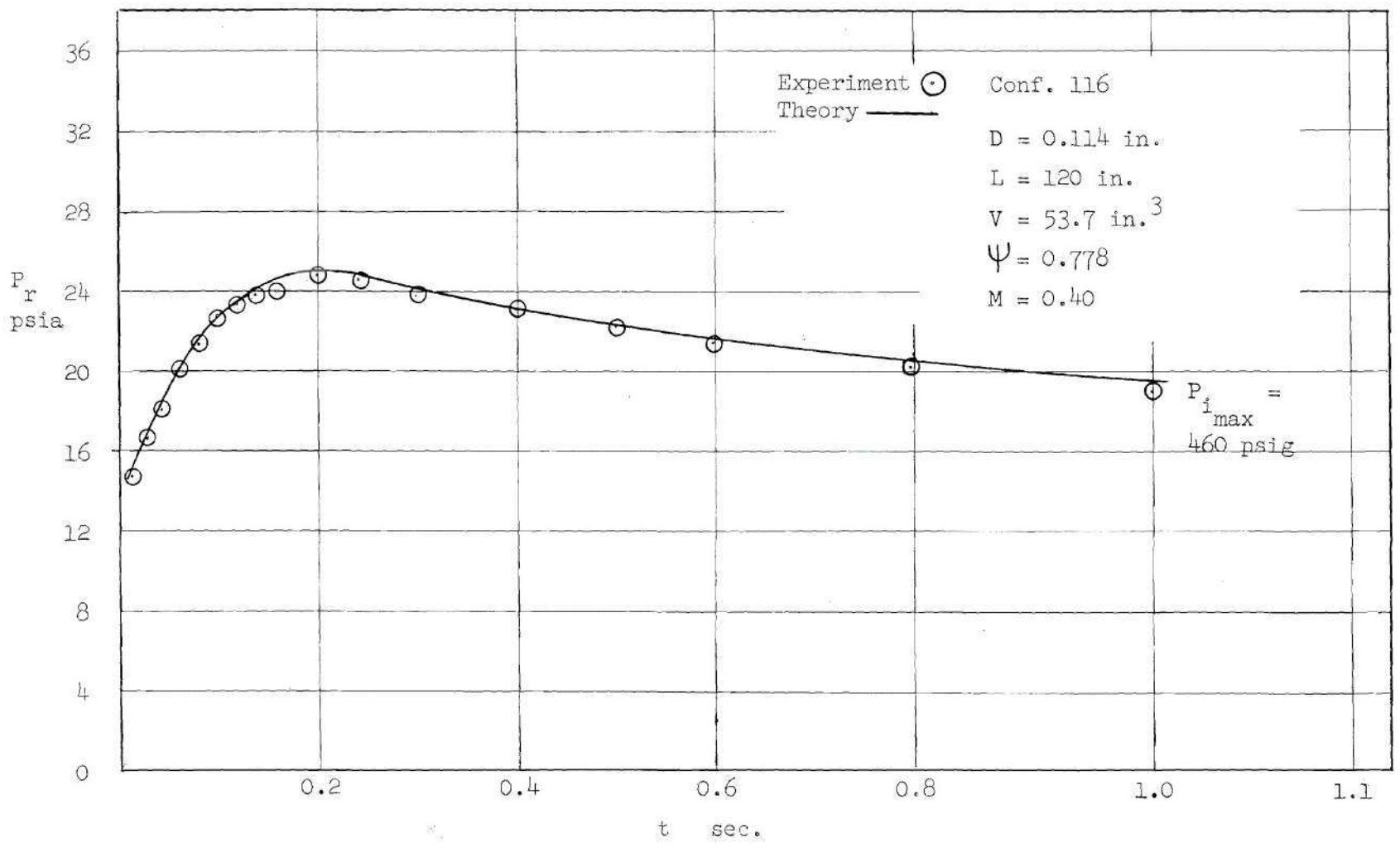

Fig. 19 Correlation of Theory with Experiment for $\Psi = 0.778$ $M = 0.40$

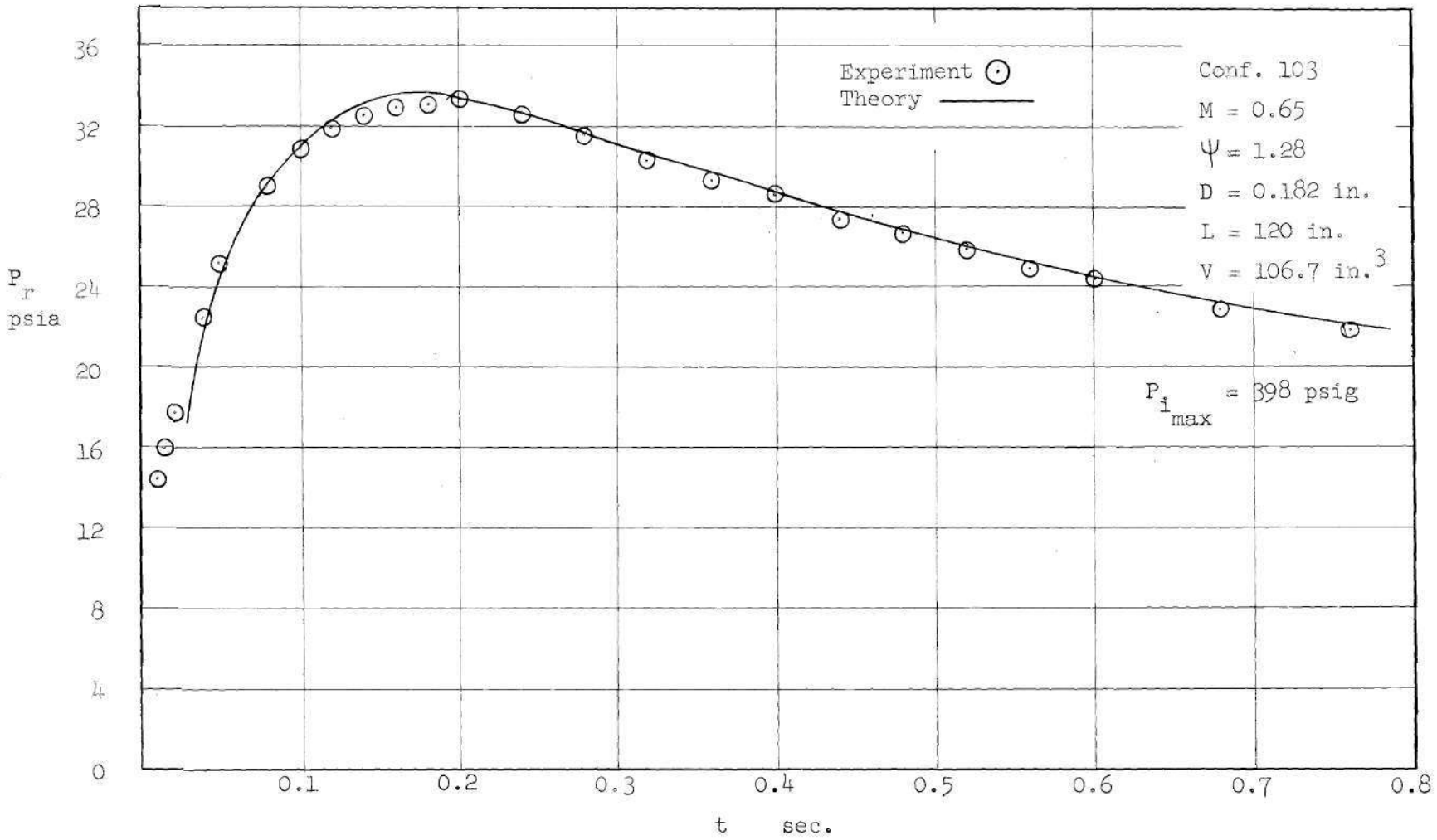

Fig. 20 Correlation of Theory with Experiment for $\Psi = 1.28$ and M = 0.65

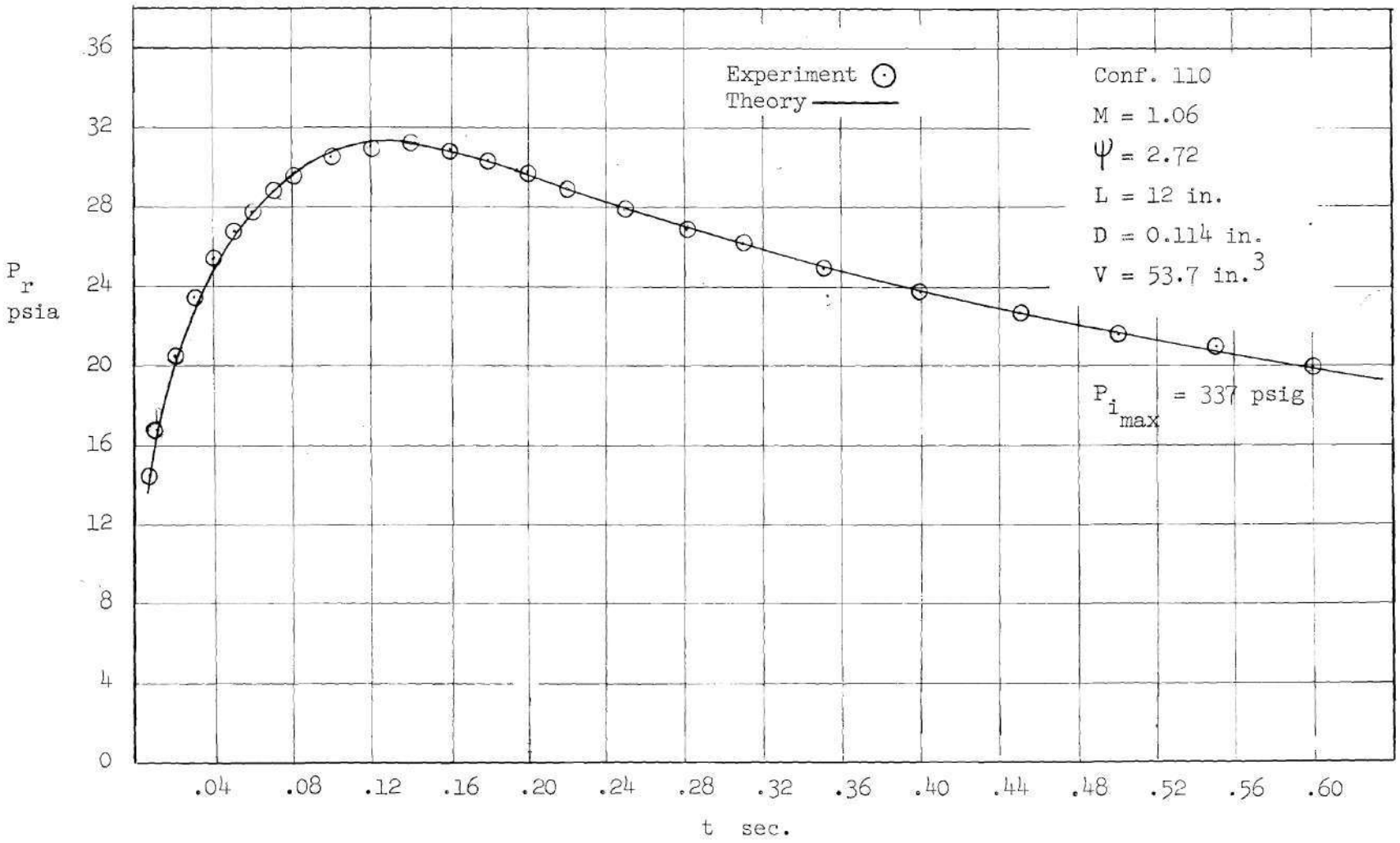

Fig. 21 Correlation of Theory with Experiment for ψ = 2.72 and M = 1.06

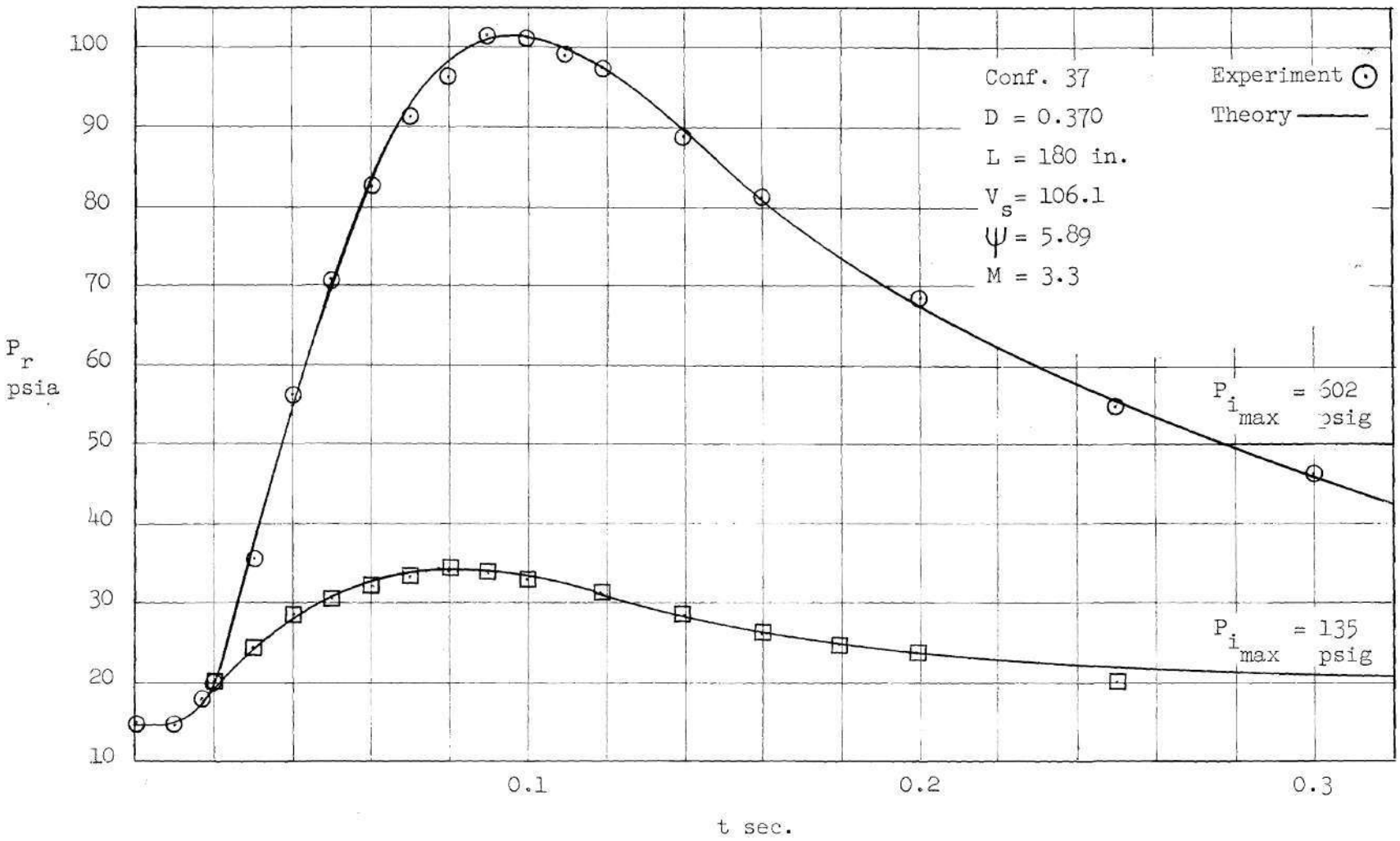

Fig. 22 Correlation of Theory with Experiment for ψ = 5.89 and M = 3.3

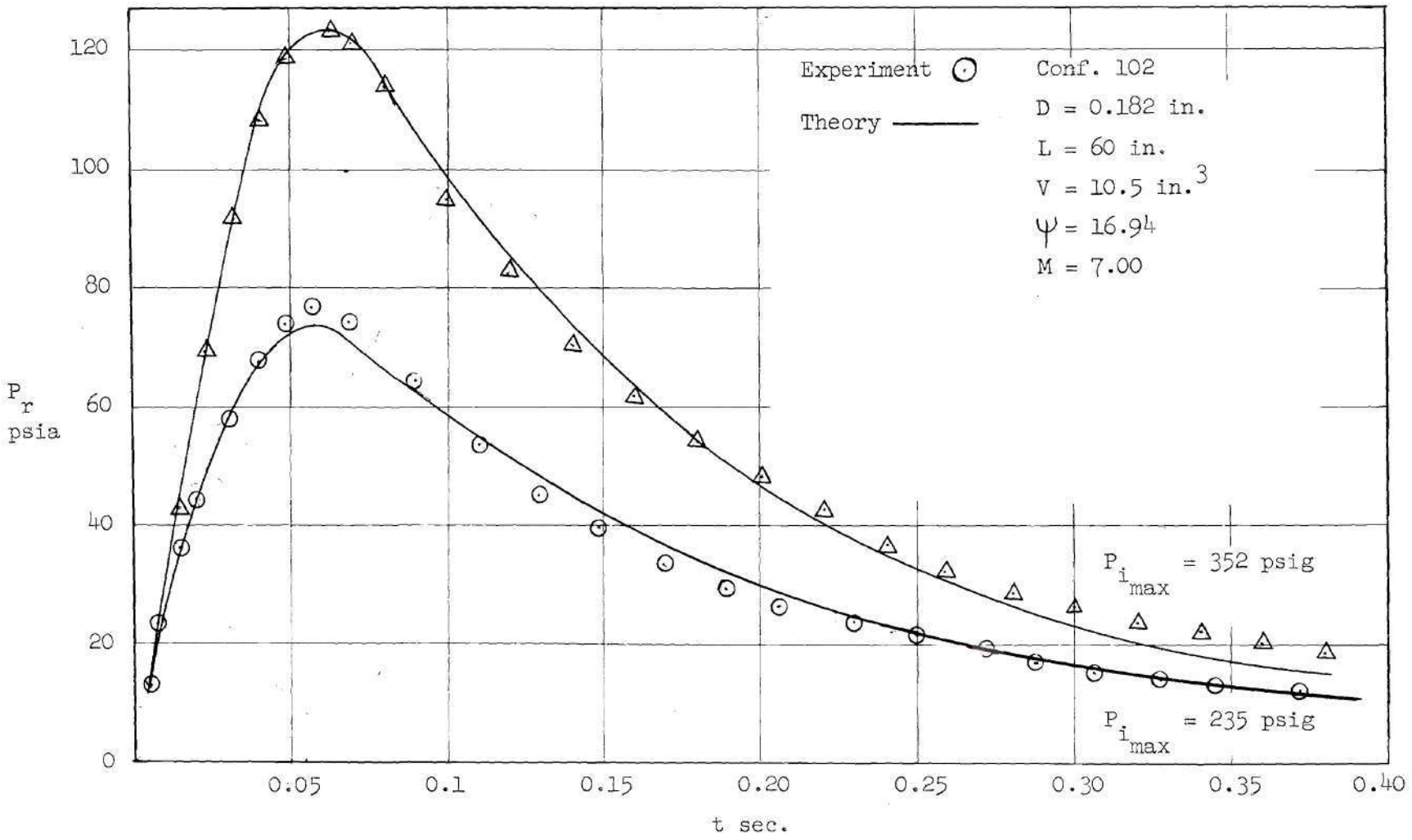

Fig. 23 Correlation of Theory with Experiment for Ψ = 16.94 and M = 7.00

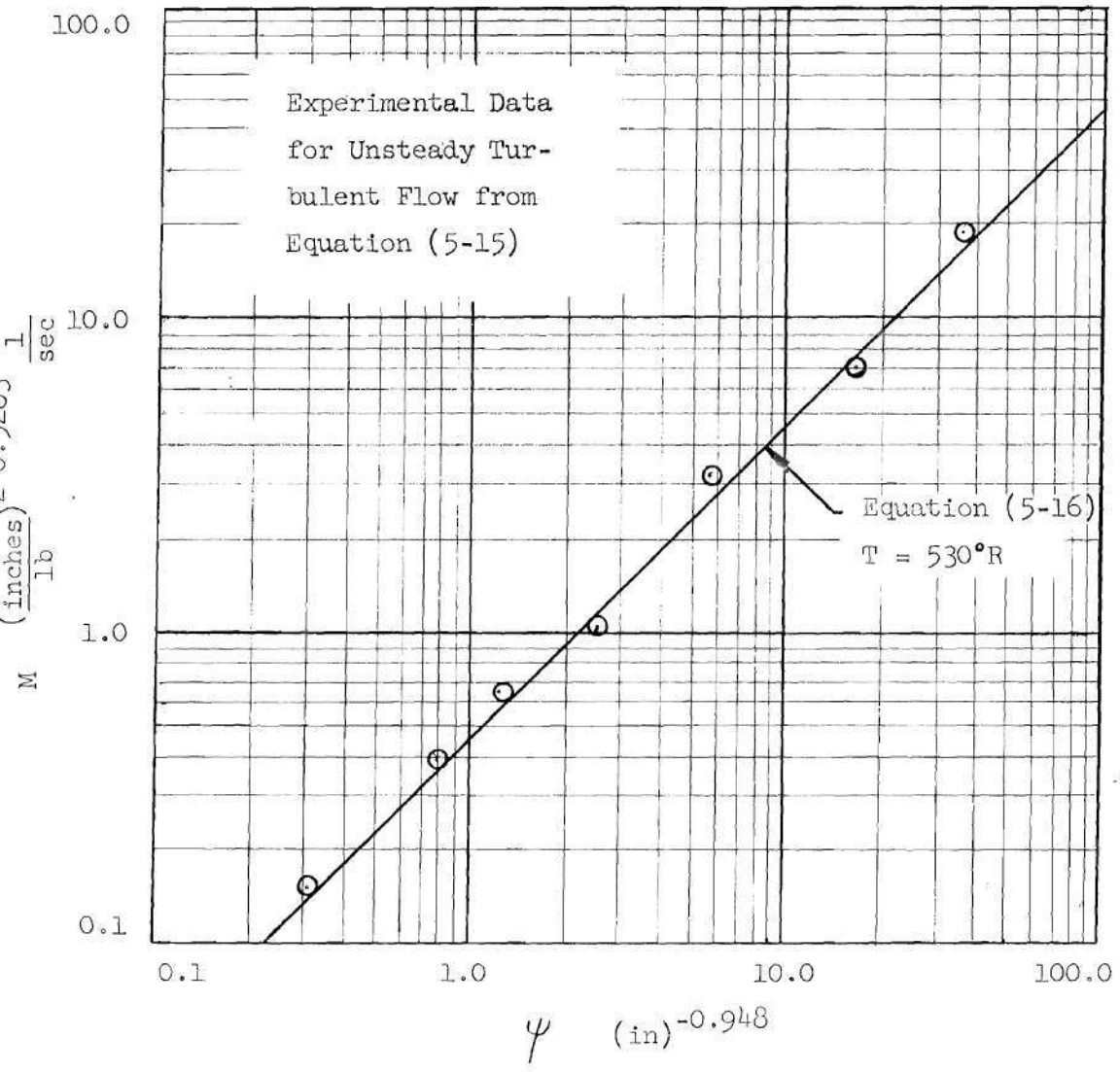

Fig. 24 System Parameter M as a Function of Geometric Parameter ψ for Turbulent Flow

an analytical expression for the input pressure and a known ambient flow temperature will yield quantitative agreement between theory and experiment.

CHAPTER VII

CONCLUSIONS

The experimental results of this investigation are limited to tube lengths from 1 to 15 feet, tube diameters from 0.114 to 0.370 inches, receiver volumes from 10 to 106 cubic inches and straight-through fitting diameters from 50 to 100 per cent of the tube diameters.

Also, the experimental results are limited to shock waves generated by the method outlined in Chapter I with strengths varying from 30 to 700 psig.

Under these restrictions, the following conclusions can be drawn from the experimental data:

1) The attenuation of the shock wave is increased with

(a) an increase in receiver volume

(b) an increase in tube length

(c) a decrease in tube diameter

(d) a decrease in fitting diameter

2) Small changes in diameter have a greater effect on the attenuation of the shock wave than a corresponding change in any one of the other geometric dimensions of the system. The theoretical results are further restricted to straight-through fitting diameters of 100 per cent of the tubing diameters and to ambient temperatures in the range of 520 to 540 degrees Rankine. Under these additional restrictions, the following conclusions are drawn:

1) The use of steady-state data in the determination of the constants C and N in Equation (5-5) gives accurate results for turbulent flow.

2) The semi-empirical relations for turbulent flow, Equations (5-13), (5-14) and (5-15), will adequately predict the transient response pressure for input pressure functions of the type examined.

CHAPTER VIII

RECOMMENDATIONS

In order to extend the theoretical and experimental results of this investigation, it is recommended that:

1) Experimental runs be made at higher shock tube pressures to determine if the linearity between $P_{r_{max}}$ and $P_{i_{max}}$ exists for shock wave strengths greater than 700 psig.

2) Experimental runs be made to determine the effect of receiver volumes of less than ten cubic inches on the shock wave attenuation.

3) Experimental runs be made for flow temperatures greater than 540°R and lower than 520°R.

4) Experiments be conducted to determine the effect on the shock wave strength and shape due to rupturing the diaphragm with different shaped firing elements.

5) Any further test runs be recorded at a paper speed of 60 to 80 inches per second in order to determine the transient input pressure more accurately.

6) Investigations be made into determining values of C and N in Equation (5-6) for various diameter reduction fittings and solutions to the resulting equations be obtained and compared with existing experimental data.

7) Solutions to Equation (5-15) be obtained for more system geometric parameters and shock wave strengths to further check the correlation of theory with experiment.

8) An accurate method be devised to measure the static temperature of the flow in the system.

9) Further investigations be conducted into the cause of the fluctations which occur in the transient input pressure.

REFERENCES

1. DeJarnette, Fred R., An Experimental Investigation of Pressure Attenuation in Typical Missile Plumbing Systems Subjected to Shock Wave Inputs - Part I, Unpublished Master's Thesis, Georgia Institute of Technology, 1958.

2. Kilburg, Richard F., An Experimental Investigation of Pressure Attenuation in Typical Missile Plumbing Systems Subjected to Shock Wave Inputs - Part II, Unpublished Master's Thesis, Georgia Institute of Technology, 1958.

3. Smith, Lester R., An Experimental Investigation of Pressure Attenuation in Typical Missile Plumbing Systems Subjected to Shock Wave Inputs - Effect of Variation of Receiver Volume, Unpublished Master's Thesis, Georgia Institute of Technology, 1958.

4. Bradley, R. G., An Experimental Investigation of Air Flow Through Insulated Tubing as a Function of Approach Temperature, Pressure Ratio, Length, and Diameter, Unpublished Master's Thesis, Georgia Institute of Technology, 1957.

5. Laster, M. L., A Theoretical and Experimental Analysis of Lengthwise Pressure Gradient for Flow in Small Bore Tubing Considering the Effect of Elevated Temperature, Unpublished Master's Thesis, Georgia Institute of Technology, 1958.

6. Lattal, Gerald L., Correlation of Pressure Losses in Small Bore Tubing for Reynolds Numbers Between 400 and 50,000, Unpublished Master's Thesis, Georgia Institute of Technology, 1960.

7. Schlicting, H., Boundary Layer Theory, Trans., Kesting, J., New York: McGraw-Hill Book Co., Inc., 1955, pp. 400-406.

8. Ducoffe, A. L., and White, F. M., Jr., A Theoretical and Experimental Study for the Prediction of Pneumatic Pressure Lag Inherent in Typical Ballistic Missile Plumbing Systems. Army Ballistic Missile Agency, Contract No. DA-01-009-ORD-595, 1959.